CHAPTER V

PROPAGATION DATA BASES

Researchers have been performing experiments to gather propagation data on millimeter-wave Earth-space links since the late 1960's, and in the process, have accumulated sizable data bases. In this chapter, we describe the various satellites used in this work, and present summary results of the significant experiments conducted in the United States. The results presented are primarily cumulative attenuation statistics, though some depolarization measurements are included as well. This is, by necessity, a limited sampling of the existing data bases. We therefore preface the data by citing additional summaries of propagation data for the interested reader.

5.1 SUMMARIES OF EXPERIMENTAL DATA

The International Radio Consultative Committee (CCIR) publishes a summary of worldwide experimental data in the Recommendations and Reports issuing from its periodic plenary assemblies. Volume V of this publication, "Propagation in Non-Ionized Media," deals with all aspects of microwave propagation--both terrestrial and earth-to-space. Within Volume V, the data is presented as a series of reports and recommendations submitted to and adopted by the CCIR. Because of this presentation format, data of interest to designers may be found in several places.

The most complete collection of measured propagation data is found in the two CCIR documents;

1. Report 564-3, "Propagation Data and Prediction Methods Required for Earth-Space Telecommunications Systems," (CCIR-1986a), and

2. Document 5/378, "Data Banks Used for Testing Prediciton Methods in Sections E, F and G of Volume V," (CCIR-1986b).

The CCIR separates the data between the two reports based on the availability of an acceptable prediction method for that type of measurement. Data for which an accepted method does not exist is presented in the first document (Report 564-3), while data for which an accepted method does exist is presented in the second document.

The data summaries in Report 564-3 are presented in Annex I, and include sections on the following subjects:

. Seasonal variations - worst month

. Duration of individual fades

- Rates of change of attenuation

- Scintillation and multipath effects

- Noise temperature

. Cross-polarization due to hydrometers

- Angle-of-arrival

Document 5/378 presents detailed tabulations of earth-space path data for:

- Annual slant-path rain attenuation statistics (Table II-l),

- Worst month slant-path attenuation statistics (Table II-2),

- Fade duration statistics (Table II-3), and
- Annual XPD statistics based on satellite measurements (Table II-4).

The results of extensive NASA sponsored measurements conducted in the 1970's is documented in a report entitled "A Compendium of Millimeter Wave Propagaiton Studies Performed by NASA," (Kaul, et al - 1977). The report contains a reasonably complete summary and references to the 15.3 and 31.65 GHz measurements with ATS-5, and the 13.2, 17.8, 20 and 30 GHz measurements with ATS-6.

5.2 SATELLITES USED FOR PROPAGATION RESEARCH

Within the United States and Canada, four satellite systems (seven satellites) have been utilized to obtain the bulk of the earth-space propagation data. A brief summary of the satellite characteristics that relate to propagation studies is given in Table 5.2-1.

European researchers used 20 and 30 GHz transmissions from the ATS-6 during the 1975/76 period when the satellite was stationed over Europe. The Italian satellite SIRIO, carrying a circularly polarized three-carrier beacon at 11.331, 11.597 and 11.836 GHz, began operation in October 1977. Finally, the Orbiting Test Satellite (OTS), launched by the European Space Agency, provided beacon transmissions at 11.575 and 11.786 GHz starting in May 1978. The Japanese have launched four satellites supporting propagation research. These are designated ETS-II, CS, BS and ECS, and carry beacons at various frequencies near 12, 20 and 34 GHz (Hayashi, et al-1979).

Satellite propagation beacons are not the only means for collecting experimental data. Radars, radiometers (fixed and sun synchronous) and low-orbiting satellites can also provide valuable data, but usually with some deficiency. A general deficiency is the lack of polarization data available from these measurement

Table 5.2-1. Satellite Parameters Related to Propagation Studies

Satellite	Launch Date	Satellite Position	Uplink Frequencies	Downlink Frequencies	Antenna
ATS-5	8/12/69	Initially over Indian Ocean, drifted to 108° W. longitude; remained spinning at 76 rpm	31.65 GHz with sidebands at ±1, ±10, and ±50 MHz from carrier	15.3 GHz with sidebands at ±0.1, ±1, *5O MHz from carrier	Linearly polarized conical horns with 20" coverage and 19.1 dB boresight gain
ATS-6	5/30/74	94° W. longitude for first year then move *to* 35" E. long. and returned to 140° W.	COMSAT Exp.: 13.19- 13.2 GHz 17.74- 17.8 GHz	COMSAT Exp.: 4.14 - 4.15 GHz 4.16-4,17 GHz NASA/GSFC Exp.: 20 and 30 GHz 8 sidetones Spaced ±180 MHz	COMSAT Exp.: Dual-frequency linearly polarized dish NASA/GSFC Exp.: 20 GHz: 6° x 9° horn 2° dish 30 GHz: similar to above
CTS	1117176	116° W.	14.0- 14.5 GHz	11.7 GHz beacon 11.7- 12.2 GHz	16° horn, RHCP for beacon
COMSTAR (satellites 01, 02, 03 and D4)	D1: 5/13/76 D2: 7122176 D3: 6/29/78 M: 2/21/81	D1: 95" W. long. 02: 95° W. long. 03: 87" W. long. 04: 127* M. long.	5.9 -6.4 GHz	19.04 and 28.66 GHz beacons 3.9 -4.2 GHz	Linearly polarized offset parabolic dishes. 19.04 GHz switched between vertical and horizontal polarization. 28.56 GHz vertically polarized. Sidebands of 28.56 GHz ±528.9 MHz (D3) ±264.4 MHz (01 and 02)
ETS-II	2/77	130" E. long.		1.7, 11.5, 34.5 GHz beacons	
SIR10	8/77	15* U. long.	17.4 GHz	11.3, 11.6, 11.9 GHz beacons	
CS	12/77	135" E. long.	27.6- 6.3 GHz 6,0 -6.3 GHz	3.95, 19.45 GHz beacons 17.9 -20.2 GHz 3.8 -4.1 GHz	
BS	4/78	110° E. long.	14.0- 14.4 GHz	11.7 GHz beacon 12.0- 12.1 GHz	
01S	5/78	10* E. long.	14.2- 14.5 GHz	11.6- 11.8 GHz beacons 11.5- 11.8 GHz	

techniques. Specifically, the expense of calibrating and operating radar systems and the attenuation saturation effect in radiometer systems limit their use.

5.3. FORMAT OF DATA PRESENTED

Because of the volume and variety of data being presented by experimenters throughout the United States and Canada, it is impossible to claim that the following data is complete. However it is certainly representative of the tropospheric effects on earth-space paths for the location indicated.,

To limit the volume of data presented, the cumulative attenuation statistics will be emphasized, since this is the most complete data base available and, from this, the rain rate and depolarization may be inferred (as described in Chapters 3 and 4). The results will be presented by frequency range or satellite beacon frequency, as appropriate.

To assist with the comparison of data from various experimenters, NASA has encouraged the use of standardized cumulative statistics plot formats. The use of these formats, given in Figures 5.3-1 and 5.3-2, will permit experimental results from different sources to be overlaid for direct comparison. The forms cover from 0.0001 to 10 percent of the total period, which should be a sufficiently large range for most applications. The attenuation scales cover from O-35 and O-45 dB, which should be sufficient to cover the link margin range of most systems. The 45 dB graph is recommended for use above 15 GHz. These same forms may be utilized for depolarization statistics if the attenuation labels are changed to cross-polarization discrimination. Each chart should be labeled with the period of the measurement, frequency, location and elevation angle. This provides, on the figure, all the information needed for comparison of data.

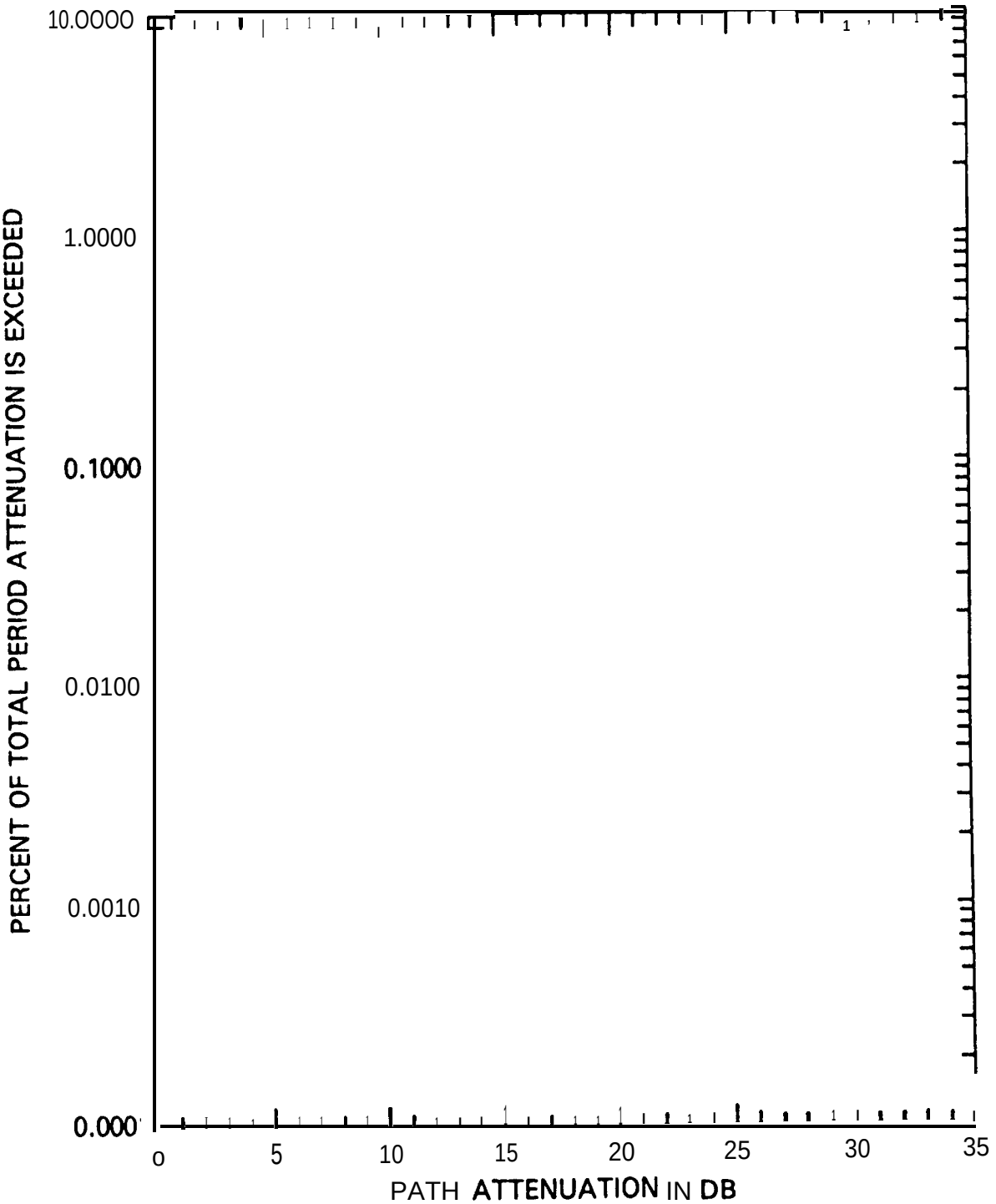

Figure 5.3-1. Cumulative Attenuation Graph for Use in the 11/14 GHz Bands

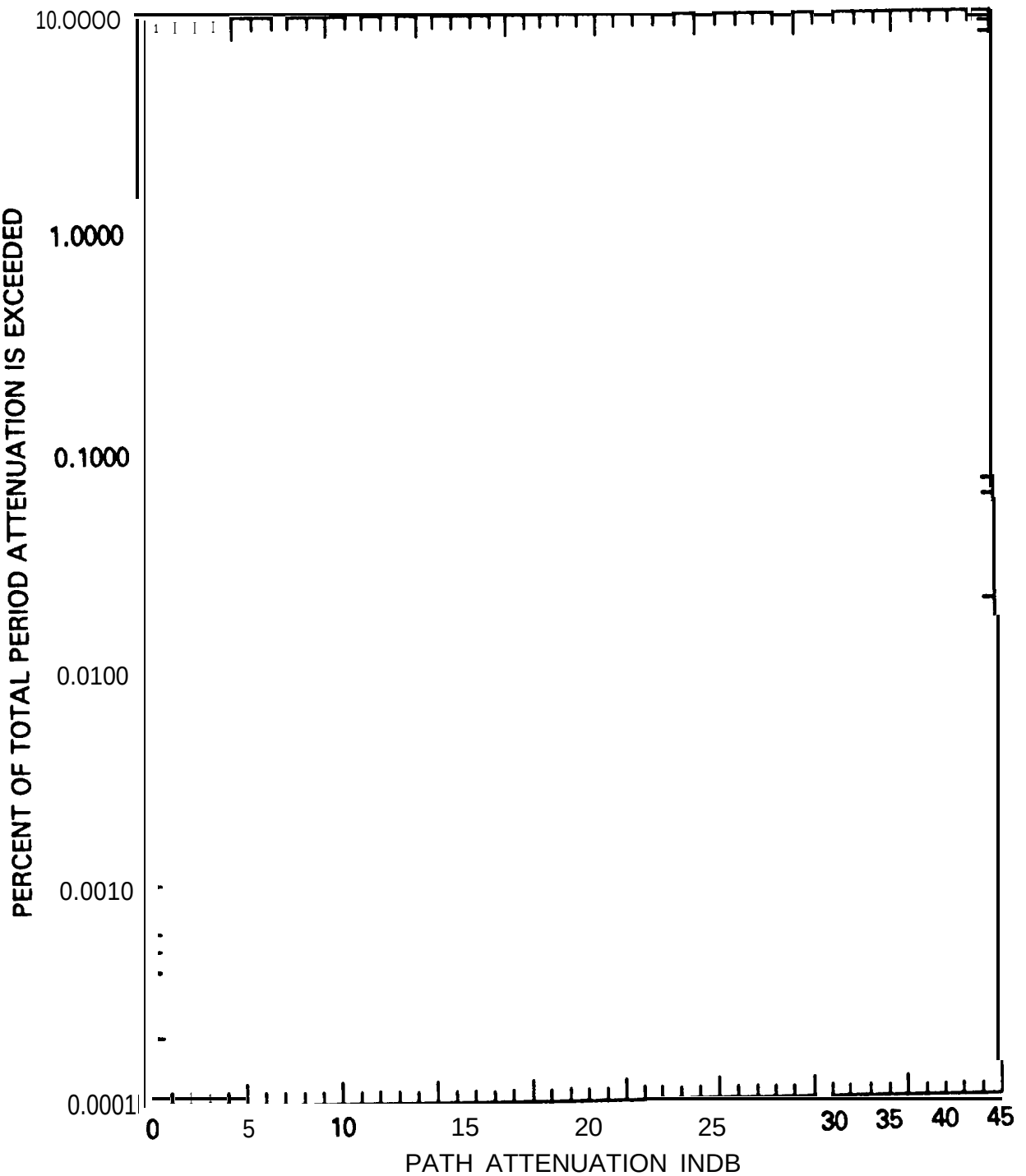

Figure 5.3-2. Cumulative Attenuation Graph for Use above 15 GHz

5.4 EXPERIMENTAL CUMULATIVE ATTENUATION STATISTICS

5.4.1 11.5-11.7 GHz Data

The Communications Technology Satellite (CTS) has provided the opportunity for extensive long-term measurements of rainfall attenuation and other propagation effects in the 11.7 to 12.2 GHz band. A continuous 11.7 GHz circularly polarized beacon operated from launch through late 1979, except for two periods during solar eclipse (March 4 through April 16, 1976 and August 31 through October 17, 1976).

Figures 5.4-1 through 5.4-5 show the cumulative statistics for the five United States locations of (listing in order of ascending elevation angle):

Waltham, MA (GTE Laboratories, Inc.)

Holmdel, NJ (Bell Telephone Labs.)

Greenbelt, MD (NASA Goddard Space Flight Center)

Blacksburg, VA (Virginia Polytechnic Institute and State University)

Austin, TX (University of Texas at Austin)

All of the distributions are based on 12 calendar months of continuous data. Details of the recording methods and processing techniques are given in the references in each figure. Table 5.4-1 summarizes the attenuation statistics at each of the locations for 0.001, 0.005, 0.01, 0.05, 0.1, 0.5 and 1% of the observation period. Note that the data shows a wide range of variations, even for consecutive years at one location.

Elevation angle differences between the five locations prevents a direct comparison of the measured distributions. The distributions can be converted to a common elevation angle by assuming the precipitation to be horizontally stratified in the

Table 5.4-1. Annual 11.7 GHz Attenuation Statistics Summary ,

LOCATION	ELEVATION ANGLE	TIME PERIOD	ATTENUATION(dB) FOR GIVEN PERCENI OUTAGE						
			1%	0.52	0.1%	0.05%	0.01%	o. 005%	0.001%
Waltham, MA	24°	Feb '77- Jan '78	<1	<1	2.5	4	10.5	14.5	(23)
		Feb '78- Jan '79	<1	<1	1.5	2.8	8.5	11	15.3
Holmdel, N.J.	27°	Jun '76- Jun '77	<1	<1	3	5	13.5	-	
		Jun '77- Jun '78	<1	<1	3	5	13.5	19.5	-
		Jun '78- Jun '79	<1	<1	2.5	3.8	9.2	12.2	29
Greenbelt, MD	29°	Jul '76- Jun '77	<1	<1	1.8	3.2	8.8	14.5	>30
		Jul '77- Jun '78	<1	1	2.1	3.8	12	18	26.4
		Jul '78- Jun '79	<1	<1	1.8	3.2	14	21	29.2
Blacksburg, VA	33°	Jan '77 - Dec '77	2	2.5	4	5	13	16.5	24
		Jan '78 - Dec '78	2	2.7	3.7	4.3	6.8	8.6	13
Austin, TX	49°	Feb '78- Jan '79	<1	1	3	5.5	13	18	23

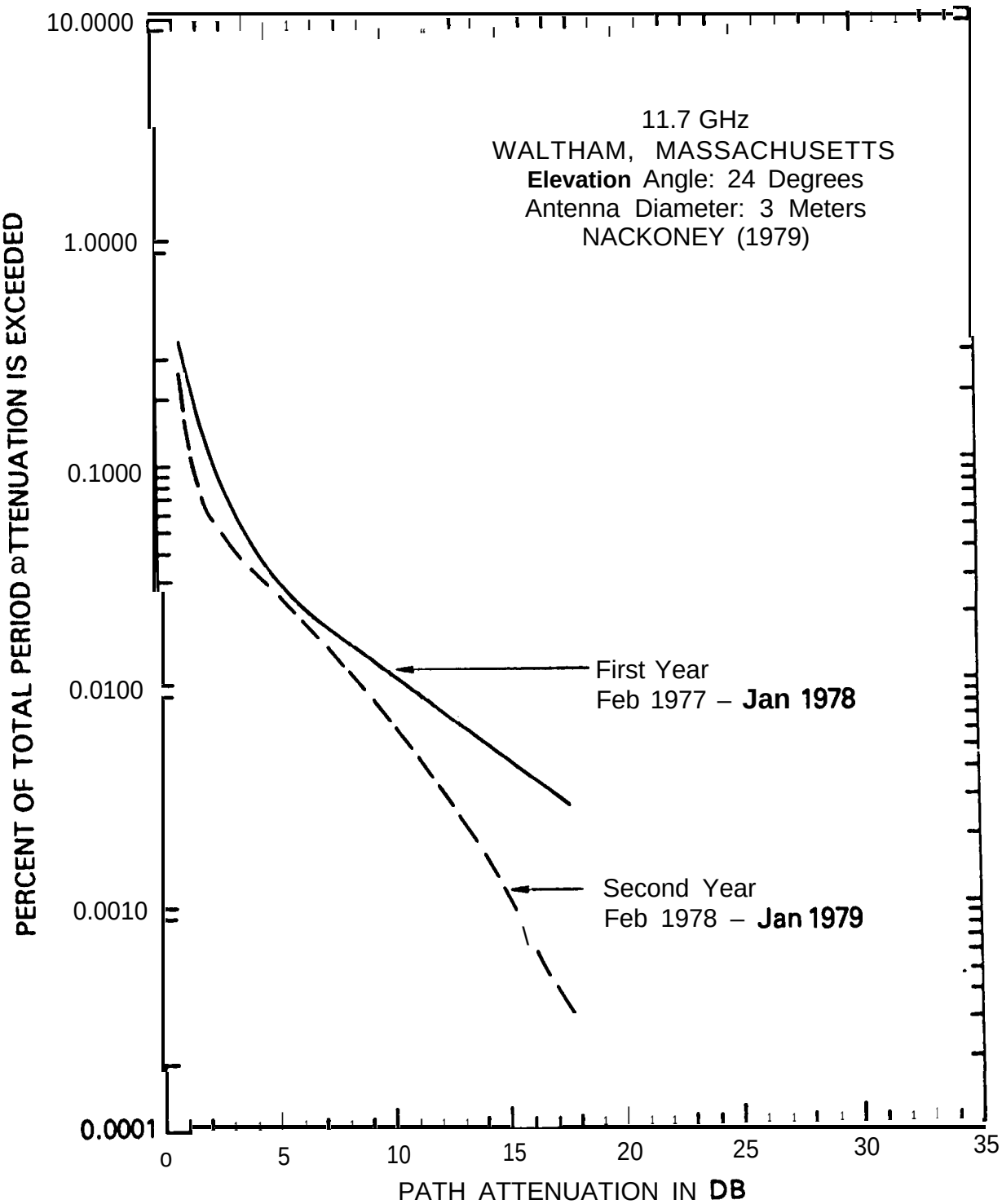

Figure 5.4-1. Annual 11.7 GHz Attenuation Distributions for Waltham, MA

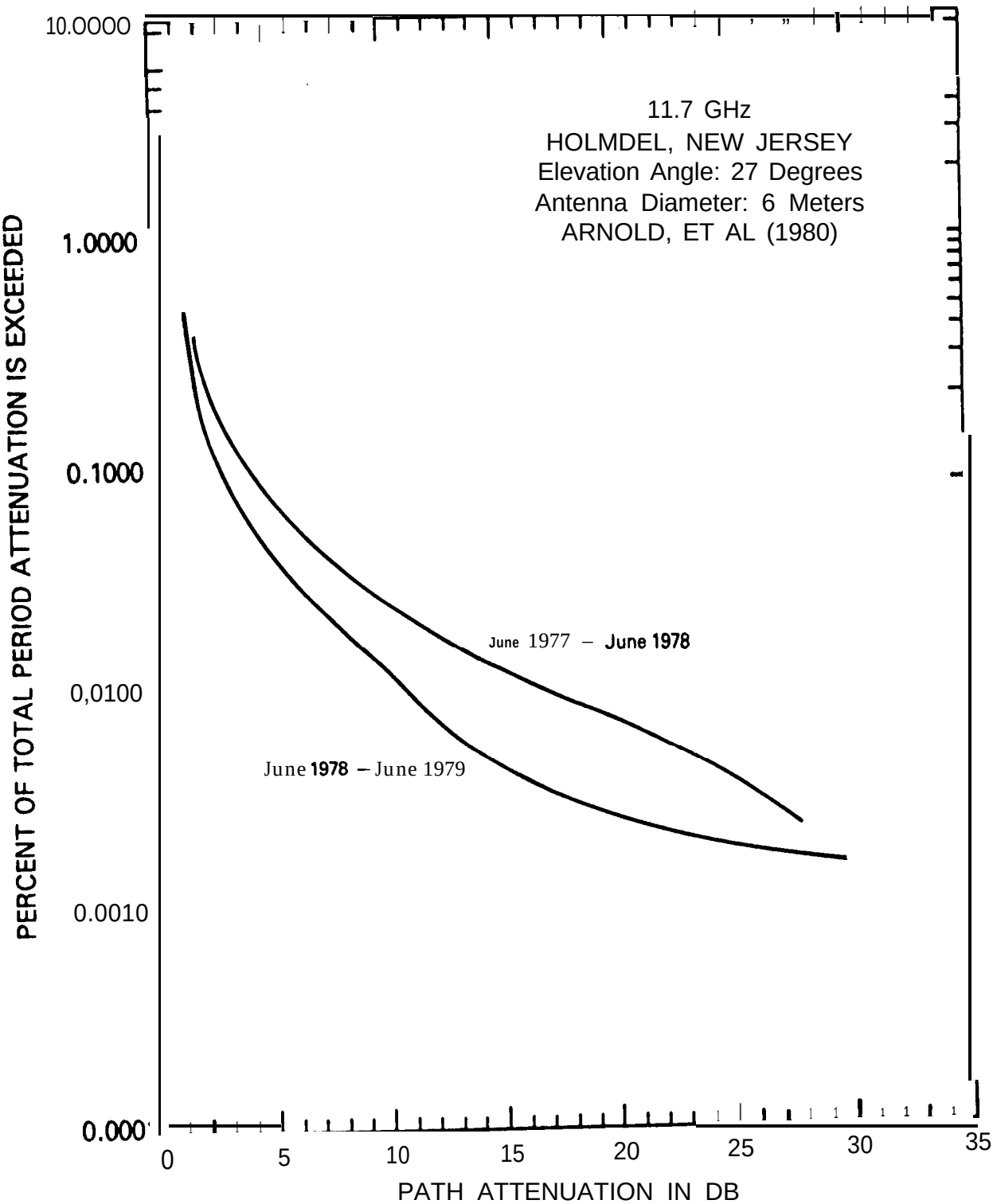

Figure 5.4-2. Anual 11.7 GHz Attenuation Distribution for Holmdel, NJ

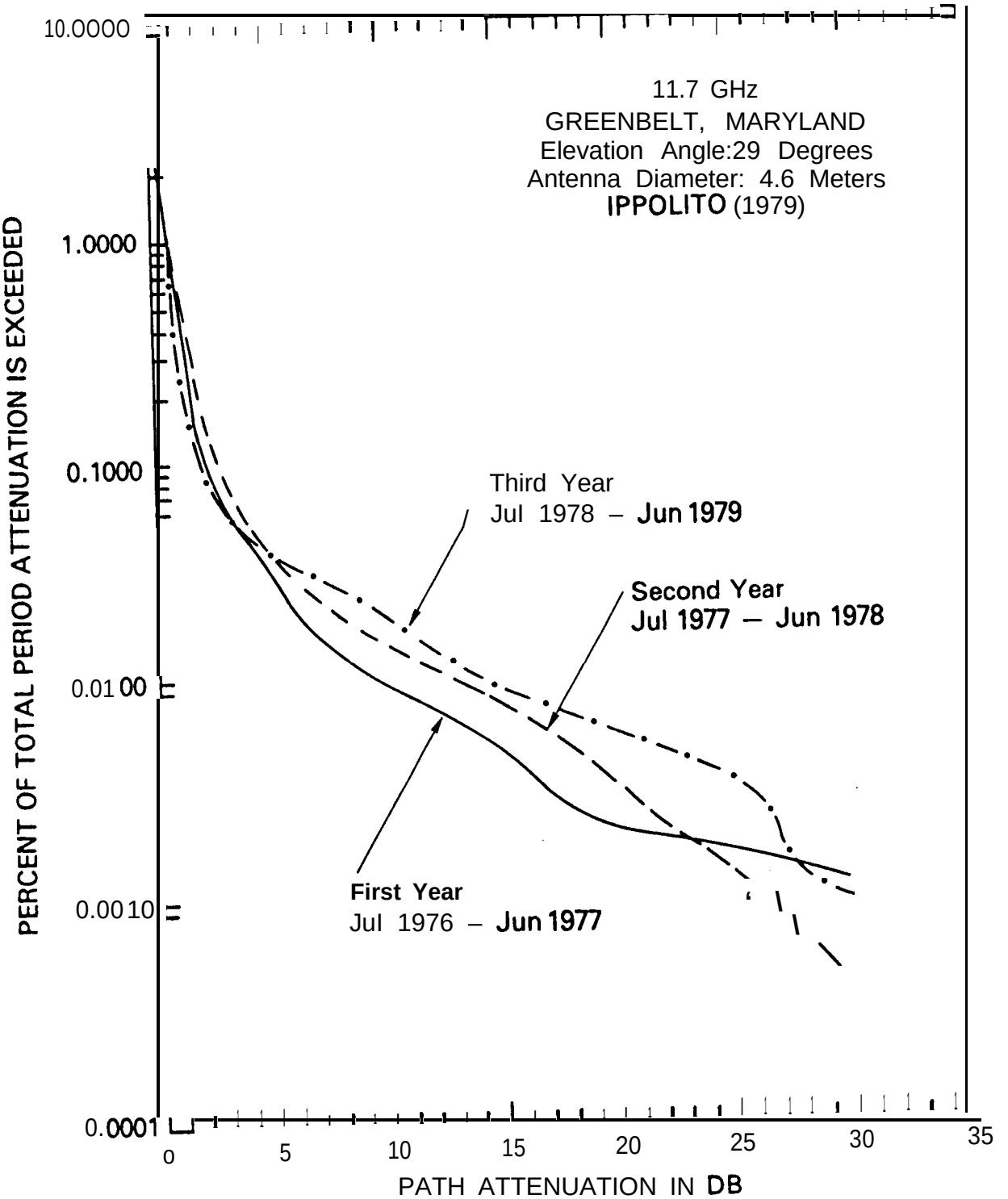

Figure 5.4-3. Annual 11.7 GHz Attenuation Distributions for Greenbelt, MD

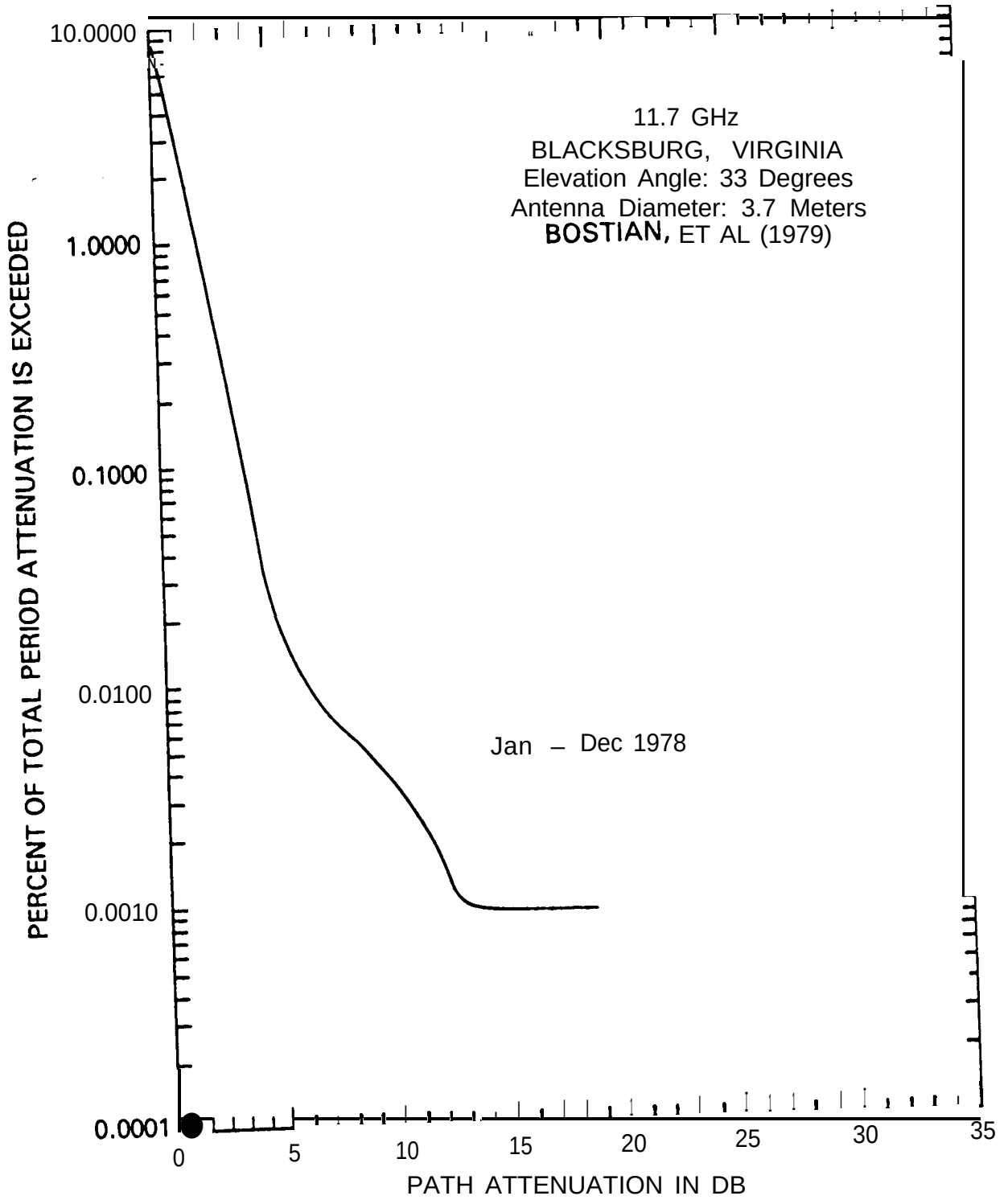

Figure 5.4-4. Annual 11.7 GHz Attenuation Distribution for Blacksburg, VA

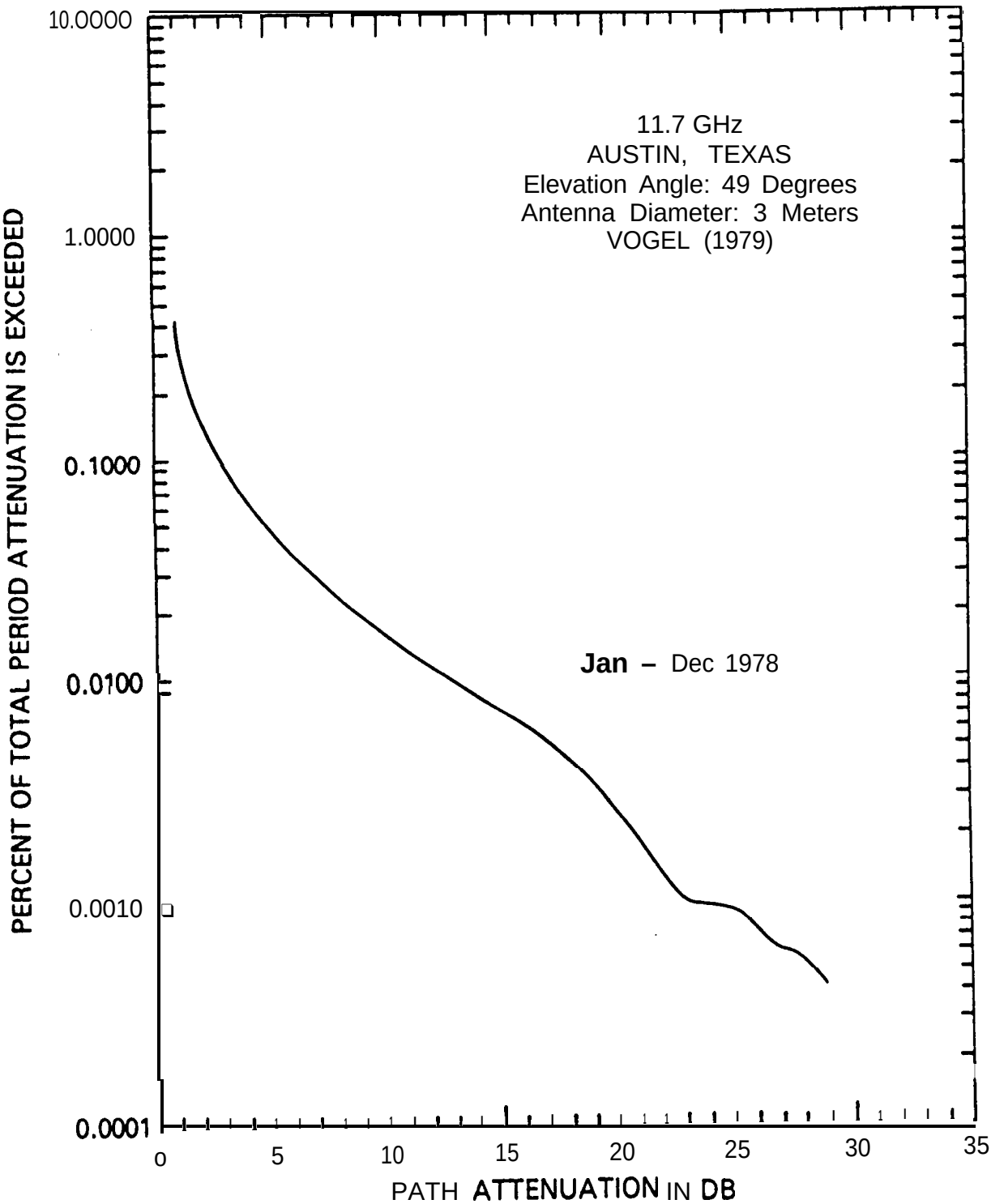

Figure 5.4-5. Annual 11.7 GHz Attenuation Distribution for Austin, TX

region of the elevation angle variations. Four of the sites have elevation angle differences of less than 9°; and, except for the 49° elevation angle at Austin, the sites differ by only a few degrees. Figure 5.4-6 presents annual 1978 distributions for each location converted to a 30 degree elevation angle. The distributions were converted to a 30° elevation angle by the relation

$$A30 = (\sin \theta / \sin 30°)\ A_\theta \qquad (5.4\text{-}1)$$

where A_θ is the measured attenuation in dB at the elevation angle θ, and A_{30} is the attenuation at an elevation angle of 30°. The distributions for the two nearest locations, Greenbelt and Holmdel, show some similarity, while the distributions for Blacksburg and Waltham are significantly lcwer. Comparisons of this kind should be observed with some caution, however, since the distributions are based on only 12 months of continuous data, and local precipitation conditions will vary greatly from year to year (see above).

It is interesting to note, however, that all five locations are in similar temperate continental rain climate regions. Both the CCIR and global rain models place the five locations discussed here in the same climate zones. Thus, attenuation prediction models based on the two above referenced procedures would yield similar attenuation distributions for all five locations. Such a similarity is not evident for the measured annual distributions presented here for those five locations.

Figure 5.4-7 presents distributions at three locations where long-term measurements, extending from 29 to 36 months duration, were available. The long-term distributions are much smoother than the individual 12 month distributions, and the curves for Holmdel and Greenbelt are very similar, particularly in the region from .01 to .0025%, which is the area of great interest for sYstem design margin criteria. The results point out the desirability for multi-year continuous measurements in the evaluation of rain attenuation effects on communications system performance.

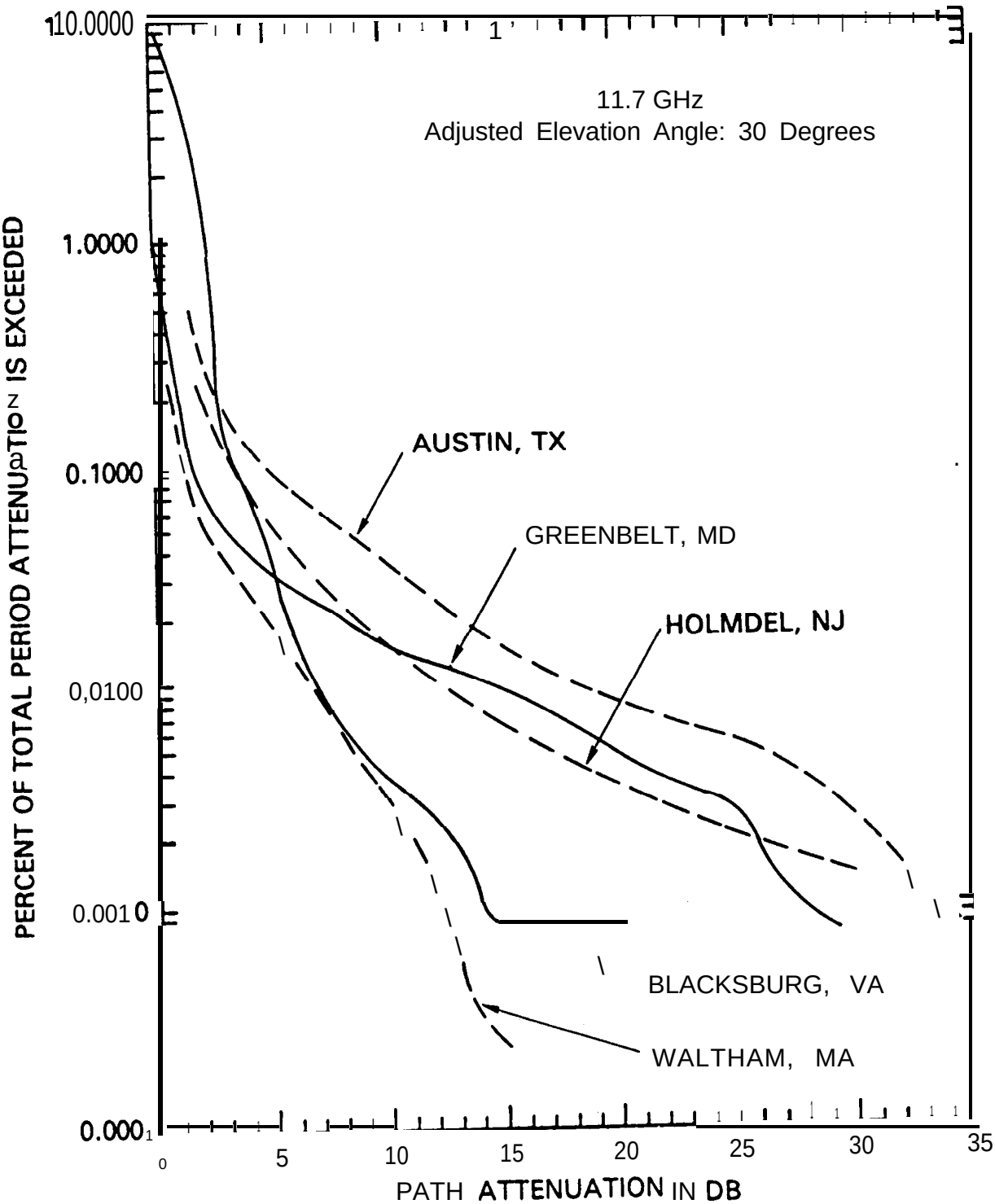

Figure 5.4-6. Comparison of 1978 Annual 11.7 GHz Attenuation Distribution of Measurements at Five Locations Adjusted to 30 Degrees Elevation Angle

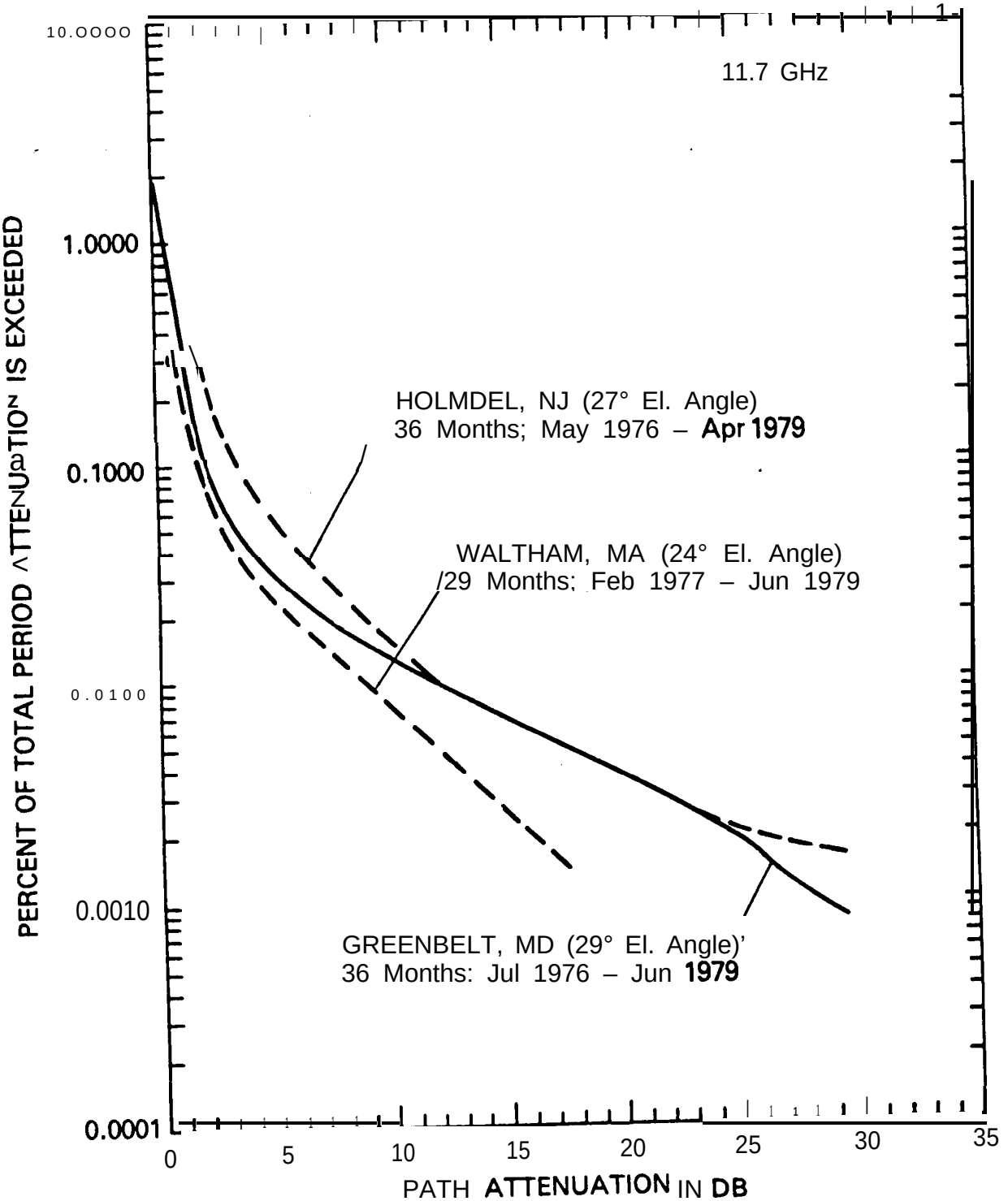

Figure 5-4.7. Long-Term 11.7 GHz Attenuation Distributions for Three Locations with Nearly Identical Elevation Angles

Representative European and Japanese attenuation data for frequencies near 11.7 GHz are shown in Figure 5.4-8 and -9. Figure 5.4-8 shows 11.6 GHz attenuation distribution curves for locations in Italy (Fucino, near Rome and Gera Lario, near Lake Como), France (Gometz-la-Ville, near Paris), and England (Slough, near London). Sources of these data are Macchiarella and Mauri (1980), Ramat (1980), and Davies (1981), respectively. Also shown is 11.5 GHz data for Japan (Kashima, on the coast east of Tokyo), from Hayashi (1979). Satellites used for the experiments represented here are SIRIO and ETS-II. Figure 5.4-9 presents data from an experiment in which separate antennas at the same station (near Darmstadt, Germany) simultaneously monitored 11.6 GHz beacon signals from the OTS and SIRIO spacecraft. The elevation angles of the two paths were within 4° of each other, but they differed by about 30° in azimuth. The large difference that is evident in the distributions has been attributed to orographic effects on local weather patterns: The SIRIO link passes over a hilly area for several kilometers while the OTS link lies over the Rhine river valley. These results (from Rucker - 1980) demonstrate the degree to which local climatic variations can affect rain attenuation statistics.

5.4.2 15-16 GHz Data

The 15 to 16 GHz experimental data base shown in Figure 5.4-10 is limited. The satellite beacon measurements were taken by NASA and COMSAT at North Carolina and Maryland. The earlier radiometer measurements by Bell Telephone Laboratories are included to supplement this satellite data. These radiometer measurements appear to agree with the satellite data up to 14 dB where the radiometer measurements stop because of sky temperature saturation. No other long-term 15 GHz data bases are known to exist in the U.S. or Canada. However, the Tracking and Data Relay Satellite System will eventually provide extensive data for 7 to 22 degree elevation angles from White Sands, NM.

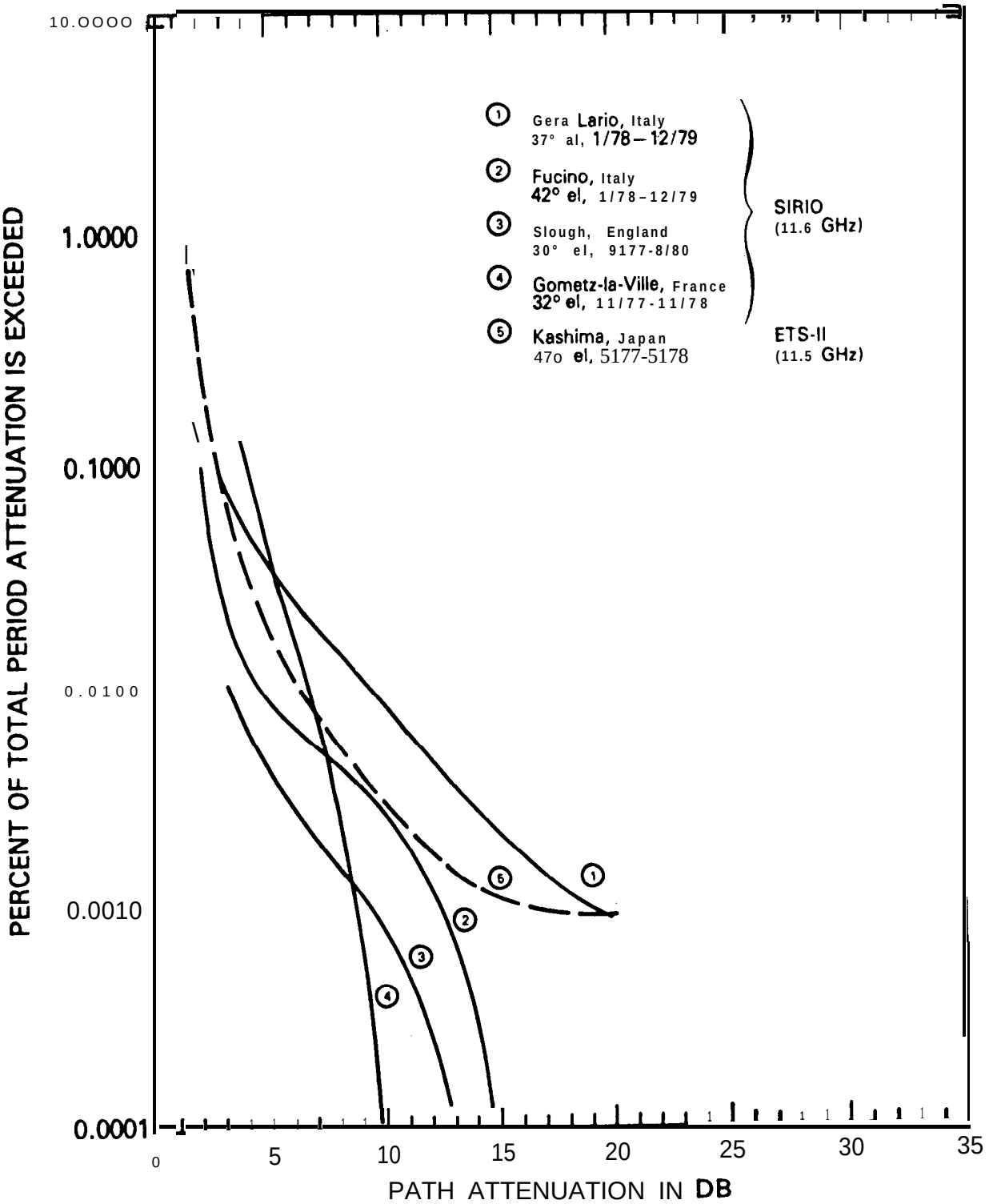

Figure 5.4-8. European and Japanese Attenuation Statistics for 11.5 and 11.6 GHz

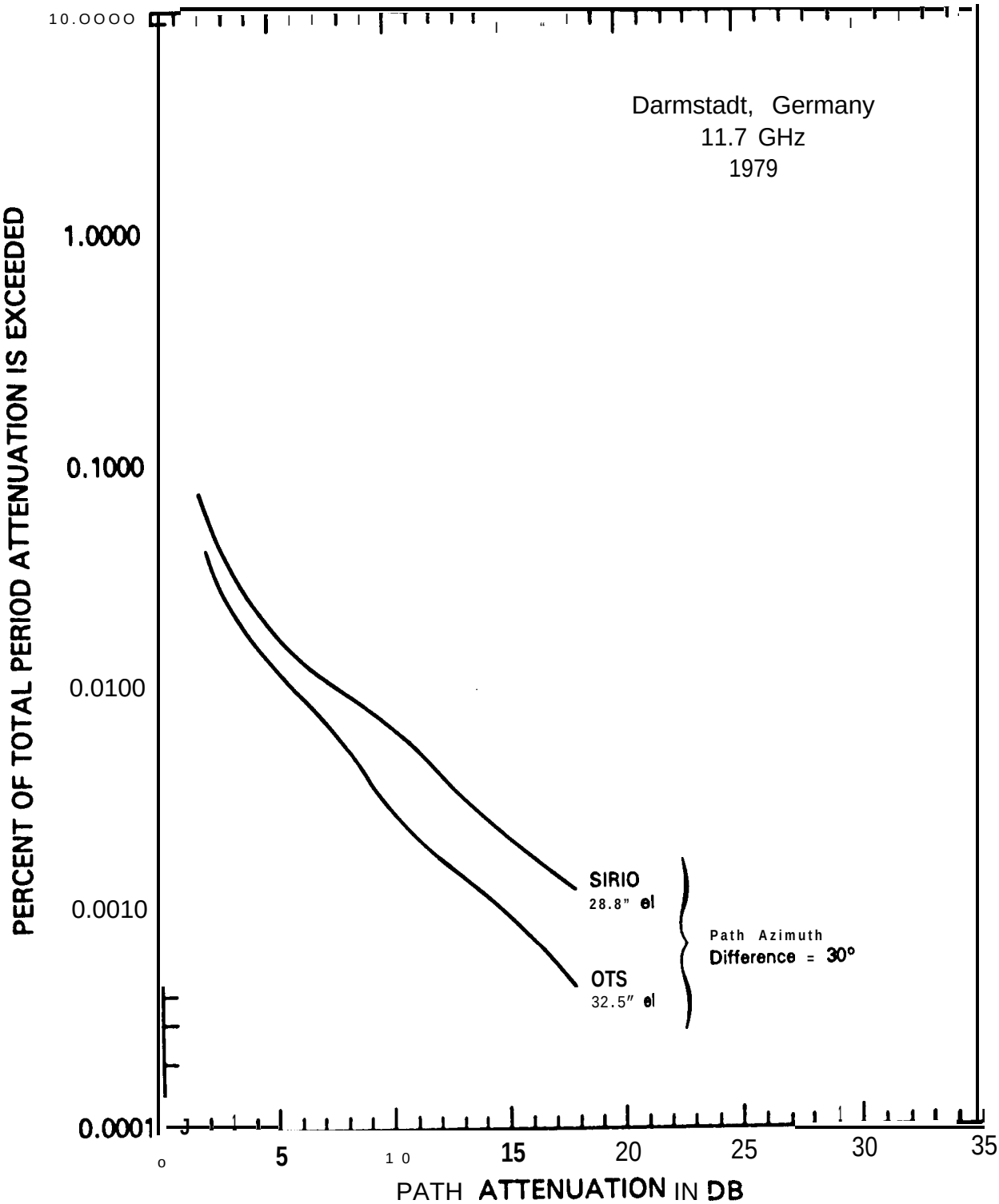

Figure 5.4-9. Simultaneous Attenuation Statistics for Two Paths from Same Earth Station

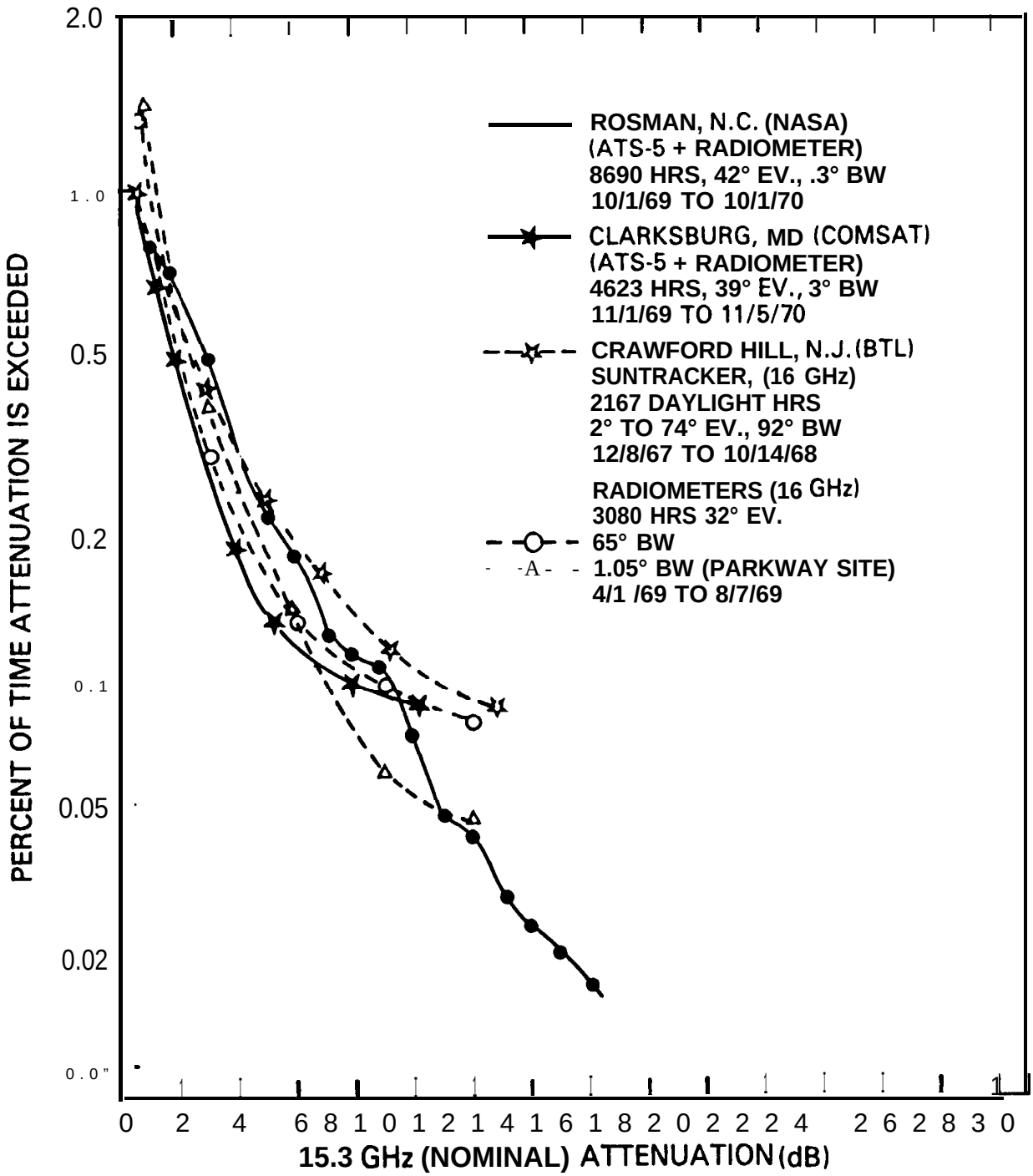

Figure 5.4-10. Summary of 15 GHz Measurements

5.4.3 19-20 GHz Data

Cumulative attenuation data in the 19 to 20 GHz range has been accumulated from both the ATS-6 and the COMSTAR beacons. In addition, the COMSTAR beacon has provided a source for direct measurement of depolarization.

The cumulative attenuation statistics at 19.04 and 20.0 GHz have been plotted in Figure 5.4-11. The Crawford Hill COMSTAR measurements (curve 2) included independent measurement of attenuation on nearly vertical (21 degrees from vertical) and nearly horizontal polarizations. Generally, horizontal and circularly polarized signals are attenuated more than vertically polarized signals. During 0.01% of the time, the COMSTAR measurements showed the horizontal attenuation to be about 2 dB greater than the vertical polarization (Cox, et al - 1979a). The polarization dependence arises because of the shape and general orientation of the raindrops. Also shown are the effects of hurricane Belle on the annual cumulative statistics. Clearly, this single event significantly shifts the curve for the moderate values of attenuation associated with heavy, but not intense, rain rates.

Figure 5.4-12 shows results from Japanese experiments using the 19.45 GHz beacon on the CS spacecraft.

5.4.4 28-35 GHz Data

The 28.56 GHz COMSTAR beacons and the 30 GHz ATS-6 beacon have provided excellent sources for attenuation measurements in the 30 GHz frequency region. The cumulative attenuation statistics for several locations in the U.S. are given in Figure 5.4-13. Japanese researchers have collected annual propagation data at 34.5 GHz with the beacon on the ETS-II satellite, as shown in Figure 5.4-12.

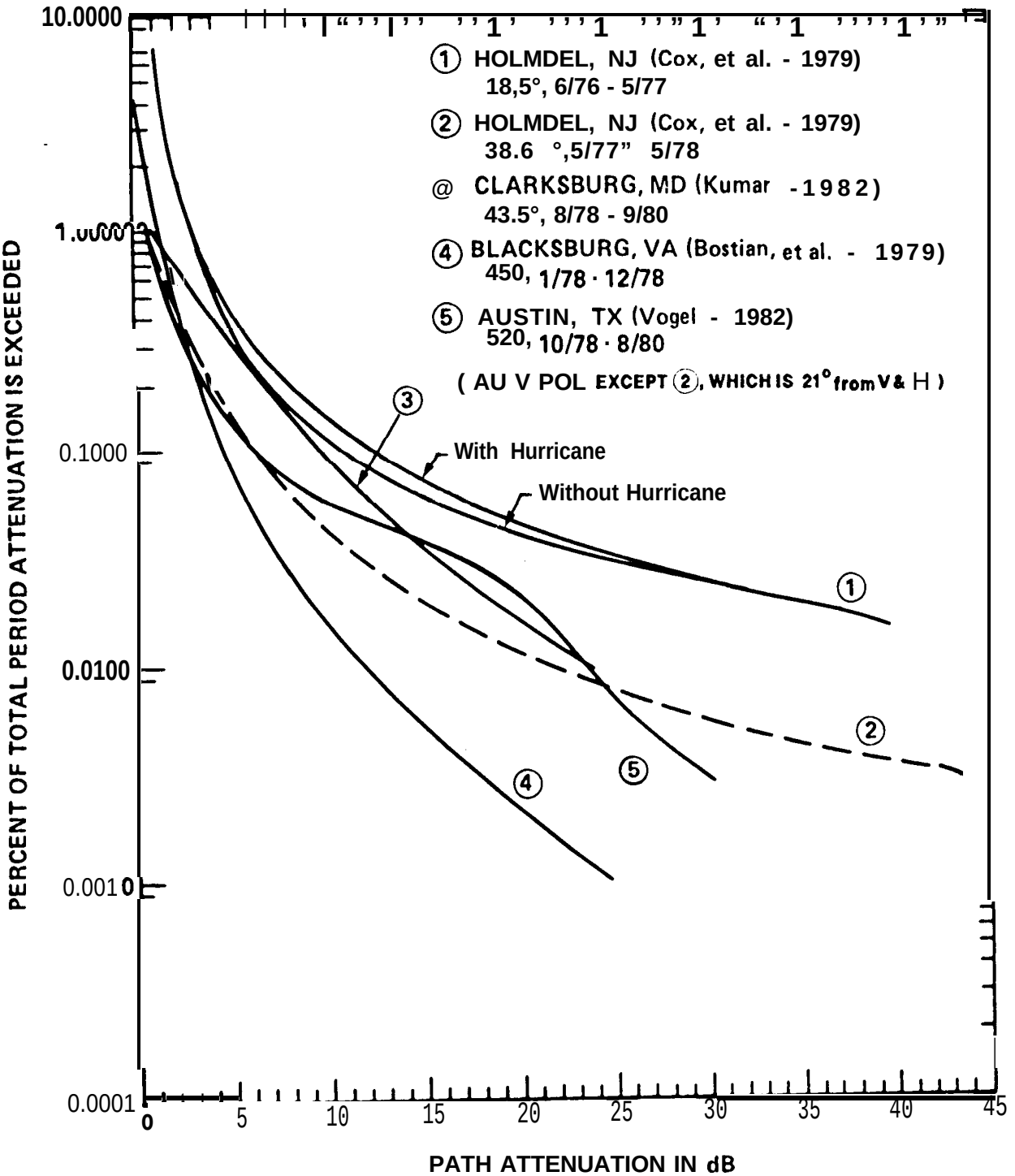

Figure 5.4-11. Summary of 19.04 and 20 GHz Measurements

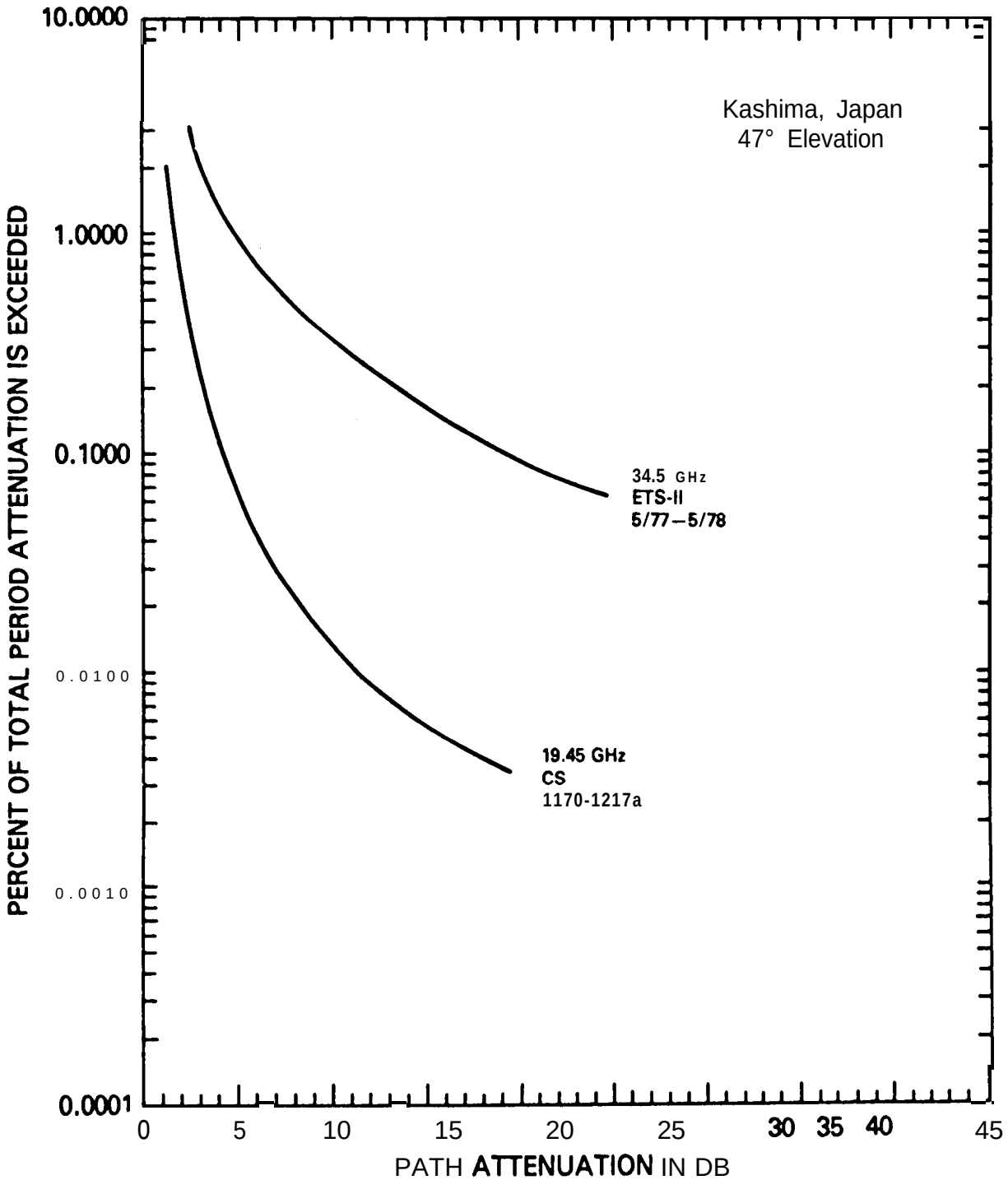

Figure 5.4-12. Results of Experiments with Japanese ETS-II and CS Beacons

5.4.5 Frequency Scaling of Attenuation Data

The relation between measured attenuations may be examined in several ways. The so-called statistical relation is obtained as a set of paired attenuations that are exceeded for equal amounts of time. These points may be obtained from the cumulative attenuation distributions. For the Crawford Hill measurements, for example, (Arnold, et al-1979) 19.5 dB attenuation at 19 GHz and 40.3 dB at 28 GHz were both exceeded for 65 min. This statistical relation is plotted in Figure 5.4-14 as a series of open circles for 19 and 28 GHz data for Crawford Hill.

The instantaneous attenuation relation may be determined from simultaneous data recordings of attenuation at the two frequencies. This instantaneous relation is also shown in Figure 5.4-14. The dashed curve indicates the median 19 GHz attenuation observed for values of 28 GHz attenuation on the abscissa. The bars in the figure indicate the span between the 10% and 90% points in the distribution of 19 GHz attenuations observed for the 28 GHz attenuation values. The quantization is 0.5 dB for the 10% and 90% points and for the median. Note that, while these results are statistical in nature as well, 'the quantity considered is the instantaneous attenuation for the two frequencies. It is evident from the figure that the statistical relation and the median instantaneous relation are essentially identical.

The dotted line on Figure 5.4-14 is the line for $A_2 = (f_2/f_1)^2 A_1 = 2.25A_1$ where A_1 is the attenuation in dB at frequency f_1=19.04 GHz and A_2 is the attenuation in dB at frequency f_2 = 28.56 GHz. The relationships between the measured attenuations depart from a frequency squared relation particularly at high attenuation. A straight line, $A_2 = 2.1A_1$ fits the data closely up to $A_1 \simeq 20$ dB but the data depart from this line at still higher attenuation. This less than frequency squared attenuation dependence is" consistent with the frequency dependence of Chu's theoretical attenuation coefficients (1974) in this frequency range. The further decrease in frequency dependence at higher attenuations is consistent with

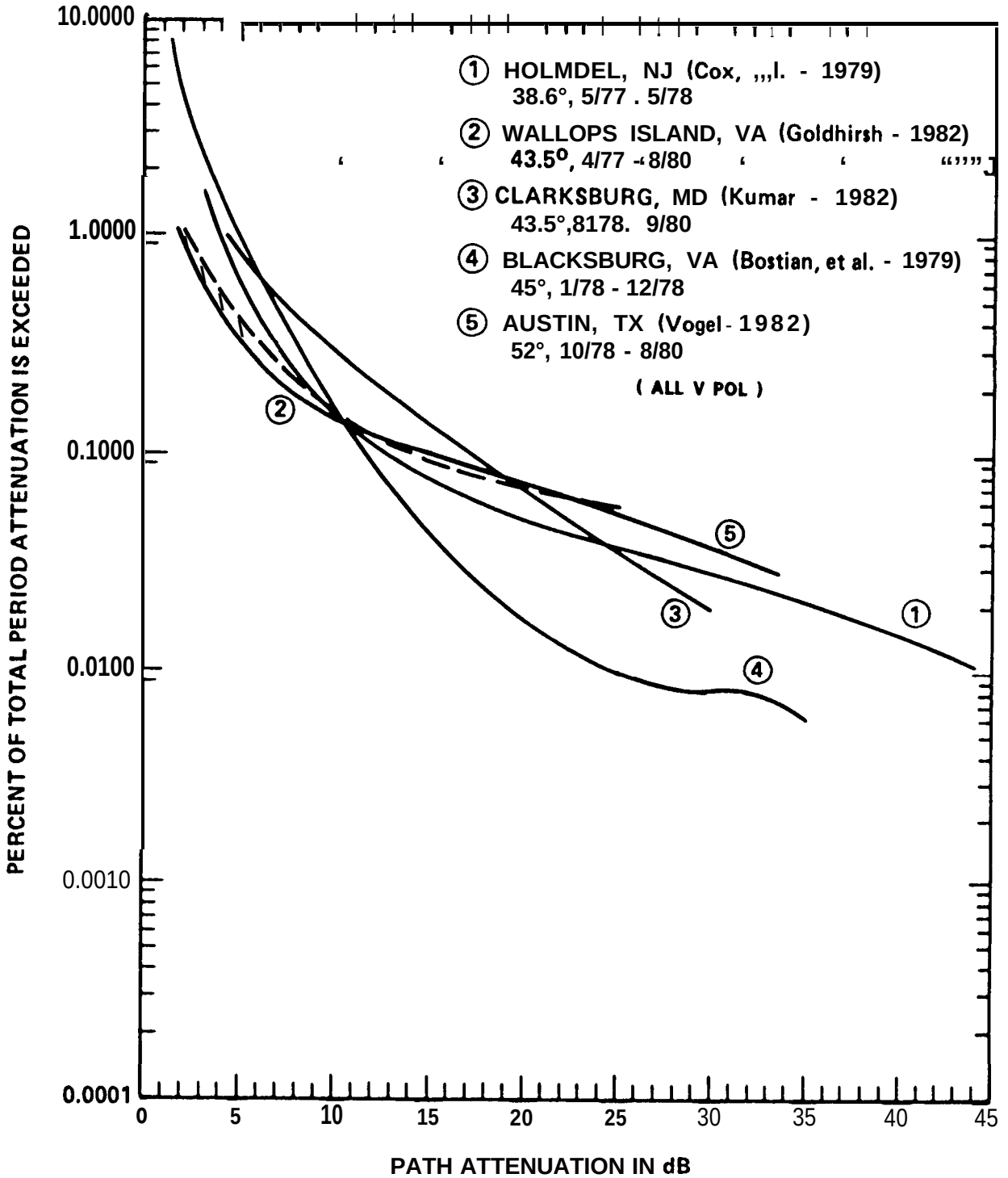

Figure 5.4-13. Summary of 28.56 and 30 GHz Measurements

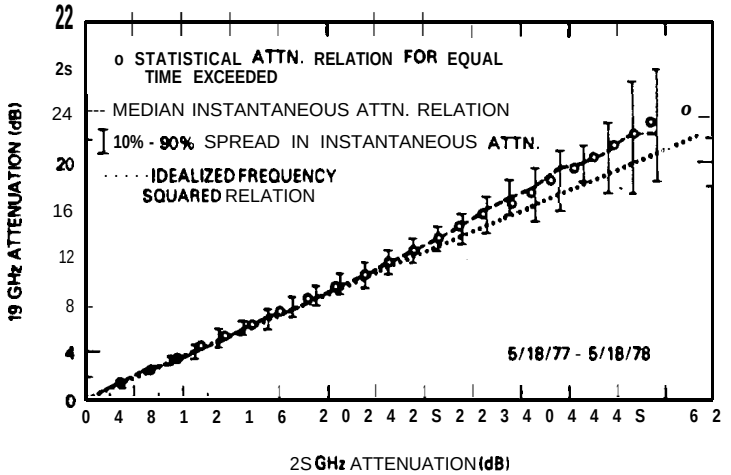

Figure 5.4-14. Relationships between 19 and 28 GHz Attenutation for Earth-Space Radio Propagation

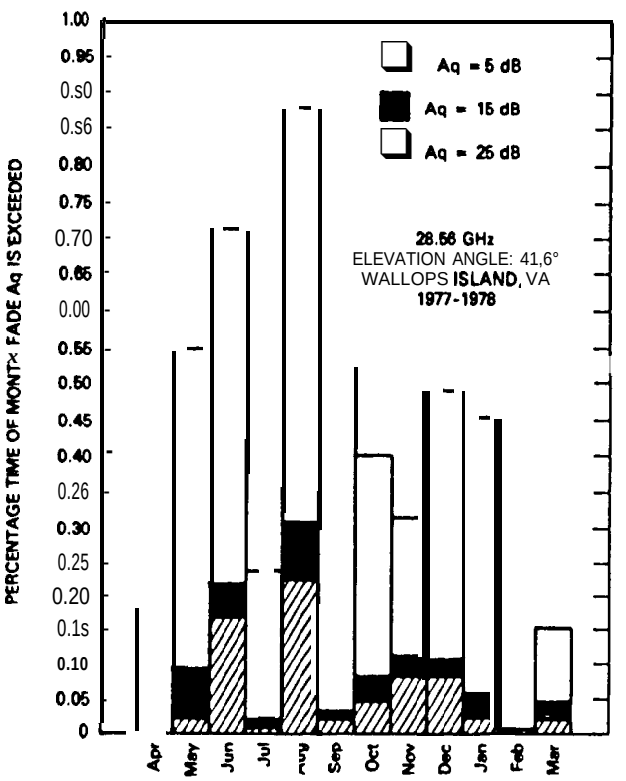

Figure 5.5-1. Histogram Denoting Percentage Times for Various Months the Fades of 5, 15,-and 25 dB Were Exceeded

the same effect observed in the theoretical coefficients at higher rain rate since higher attenuation is associated with more intense rain.

In Figure 5.4-14, the increase in the spread between 10% and 90% points as attenuation increases is consistent with constant fractional fluctuation in the ratio of the attenuations at the two frequencies.

5.5 TEMPORAL DISTRIBUTION OF FADES

Systems may be able to accommodate fades during certain months or periods of the day more readily than during other periods. To help assess the magnitude of these effects along the eastern U.S. coast, Goldhirsh (1979, 1980) and others (Rogers and Hyde - 1979, Brussaard - 1977) have prepared histograms and cumulative distributions for various-months and times.

5.5.1 Monthly Distribution of Attenuation

Figure 5.5-1 shows the percentage of time for each month in the period April 1977 to March 1978 that fades of 5, 15, and 25 dB were exceeded. These measurements (Goldhirsh - 1979) were made at 28.56 GHz from the COMSTAR D2 satellite to Wallops Island, VA at an elevation angle of 41.6 degrees. The fades are more excessive during the summer months, except for July. This low value for July is not expected to be representative for that month and demonstrates how data from a single year can misrepresent the long-term average value.

Weather Bureau data may also be utilized to obtain this distribution by month, but this procedure may be inaccurate because the type of rain may vary significantly throughout the year. Some consideration to the amount of rainfall occurring in thunderstorms in a given month is needed to make these estimates more realistic. Ideally the rain rate distribution for each month would be required along with the attenuation models presented in Chapter 3. The variability of the statistics from year to year is demonstrated by a

comparison of the 1977-78 data with that obtained at' Wallops Island in the September 1978-August 1979 period, using the COMSTAR D3 satellite (Goldhirsh - 1980). While the overall attenuation exceedance plots for the two periods agreed closely, several monthly exceedance values differed greatly between years. The percentage of July for which 15 dB was exceeded, for example," was about 0.3% in the 78-79 period compared with 0.02% in the 77-78 period. The 15 dB exceedance percentages differed by more than a factor of two between years for six of the twelve months.

5.5.2 Diurnal Distribution of Attenuation

One would expect severe fades to be most likely to occur during the late afternoon and early morning hours, when tropospheric heat exchange is the greatest and convective rains are most frequent. The 28 GHz COMSTAR data taken at Wallops Island, shown in Figures 5.5-2 and 5.5-3 (Goldhirsh - 1979), tends to confirm the expectation for the late afternoon. The figures show the attenuation statistics for the 1977-1978 period in terms of which 4-hour intervals of the day the attenuation was recorded. Figure 5.5-2 is a histogram giving time percentages for exceedance of 5, 15 and 25 dB attenuation values, and Figure S.5-3 shows the complete cumulative distributions for each interval.

The time-of-day attenuation histogram of Figure 5.5-4 is from 11.7 GHz radiometer-based attenuation data at Etam, West Virginia (Rogers and Hyde - 1979). It shows two periods of the day dominated by deep, long fades, in early morning and late afternoon, as expected. The 11.4 GHz diurnal fade distribution given by Brussaard (1977) for a number of European locations exhibits a marked peak between 1500 and 1800 local time, but no peak in the morning. The 19.5 GHz 1979-80 data for Kashima, Japan shows a very different pattern (Fukuchi, et al - 1981), including a drop in deep fades at around 1700 local time. one-year data compiled at Palmetto, Georgia using the COMSTAR 19 GHz beacon, shows a broad minimum in the diurnal distribution of deep fades between about 0500 and 1000, and a broad peak between 1700 and 2300 (Lin, et al - 1980).

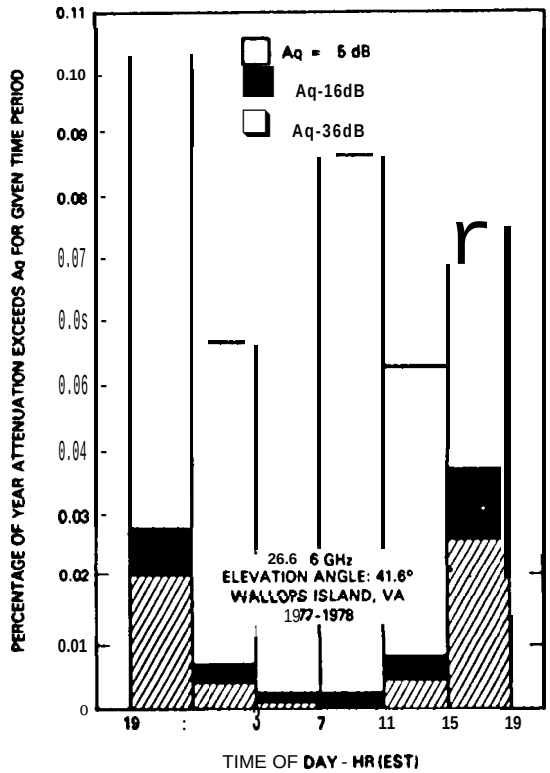

Figure 5.5-2. Diurnal Distribution of Fades Exceeding 5, 15, and 25 dB for Six Contiguous Four-Hour Time Slots of the Day

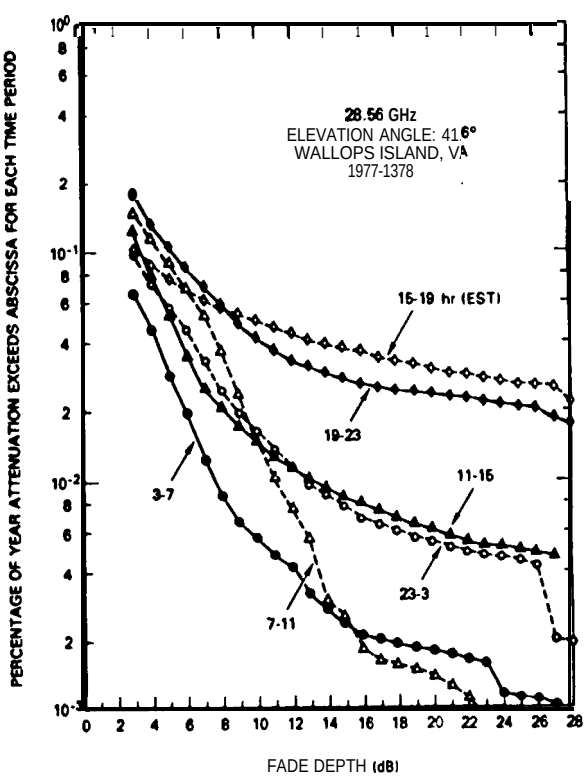

Figure 5.5-3 Cumulative Distributions for Six Contiguous Four-Hour Time Slots of Day

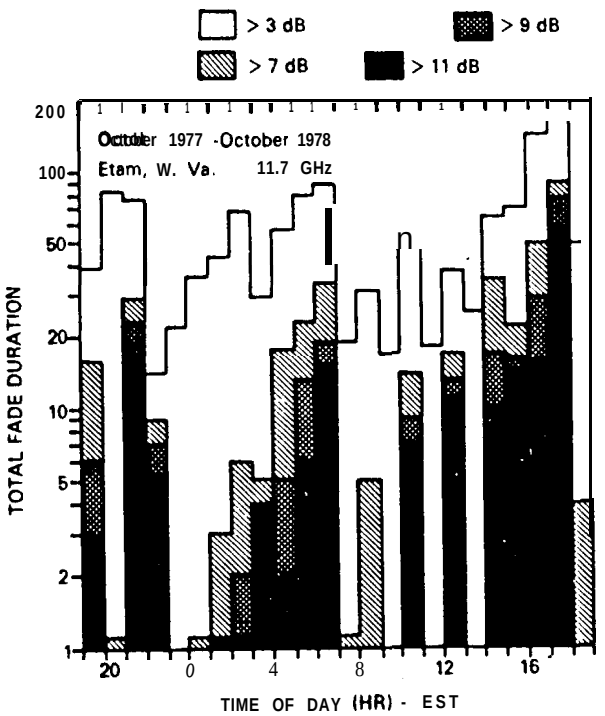

Figure 5*5-4. Diurnal Distribution of Fades Exceeding 3, 7, 9, 11 dB

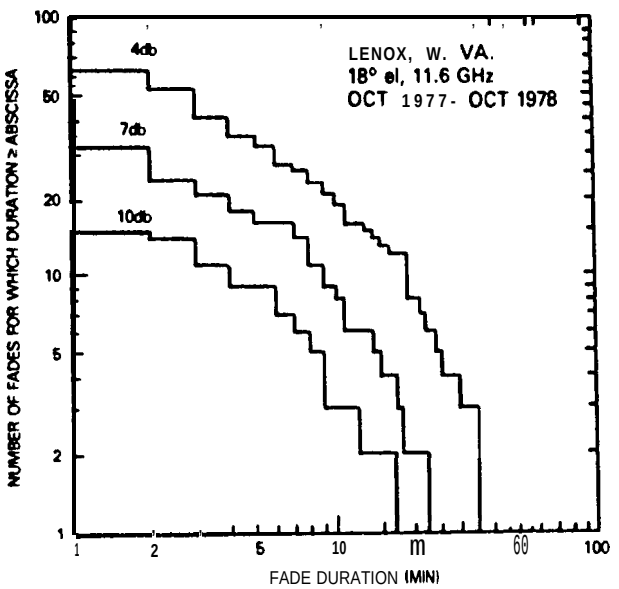

Figure 5.6-1. Histogram of Fade Duration From Radiometer Data

The diurnal distribution, like the monthly distribution, varies widely from year to year. Goldhirsh (1980) presents a comparison of diurnal distributions of the 1977-78 and the 1978-79 periods for 28 GHz attenuation at Wallops Island. In three of the six time intervals, the 15 dB exceedance percentage differed by more than a factor of two between the years.

5.6 FADE DURATION

Several experimenters have derived fade duration statistics for earth-space links. Rogers and Hyde (1979) present histograms of the number of fades exceeding specific depth and duration for 11.6 GHz at Etam and Lenox, West Virginia, based on a year's radiometer measurements. Figure 5.6-1 shows the Lenox histogram. Rogers (1981) gives similar data for Shimotsui, Japan, and in addition shows joint fade duration histograms for pairs of diversity sites in West Virginia and Japan.

Fade duration statistics have been compiled for 19 and 37 Gz at Slough, England, using a sun-tracking radiometer. Figure 5.6-2 shows histograms for fades exceeding 5 and 10 dB from the Slough data. Note that the method of presentation differs from that of Figure 5.6-1. The data in the earlier figure was the number of - fades greater than or equal to the abscissa value, and the present figure gives the number with a length falling in one-minute intervals.

The use of a sun-tracking radiometer to estimate long-term path attenuation provides a greater range of measurement than a stationary sky-noise radiometer, but the data by necessity includes no night-time fading events. Also, due to the dependence of rain attenuation on elevation angle, a rainstorm occurring when the sun is low in the sky would produce deeper fades than an identical storm occurring closer to noon. Thus, long-term attenuation data from a sun-tracking radiometer is colored by the time of day that events producing fades tend to occur. One would expect this to limit its accuracy in describing statistics for a fixed elevation angle.

Fade duration statistics from direct attenuation measurements have been compiled by Japanese researchers for 11.5 and 34.5 GHz using the ETS-11 satellite, shown in Figure 5.6-3, as well as limited 19.45 and 11.7 GHz statistics from the CS and BS experiments (Hayashi, et al - 1979).

Lin, et al (1980) present a summarization of fade duration data for 19 and 28.5 GHz on the COMSTAR (D2)-to-Palmetto, Georgia path. The durations of fades exceeding each of several attenuation thresholds between 5 and 25 dB at each frequency were normalized and presented on a single plot. The normalization consisted of dividing each fade duration value by the average duration for its frequency and threshold. The combined normalized data was shown to closely fit a log-normal distribution, which confirmed expectations.

5.7 EXPERIMENTAL DEPOLARIZATION DATA

The crosspolarization discrimination not exceeded for a given percentage of time, in decibels, is approximated by a relation (Nowland, et al-1977)

$$XPD = \tilde{a} - \tilde{b} \log_{10} (CPA) \qquad (5.7\text{-}1)$$

where CPA is the copolarized attenuation value in decibels exceeded for the same percentage of time. This suggests that the data be presented in a semilogarithmic format wherein each parameter is already a logarithm of another parameter. Therefore, in this Handbook we have replotted the results of others in order to present a uniform format of the data and to allow easy comparison with the CCIR approximation (see Eq. 4.3-27).

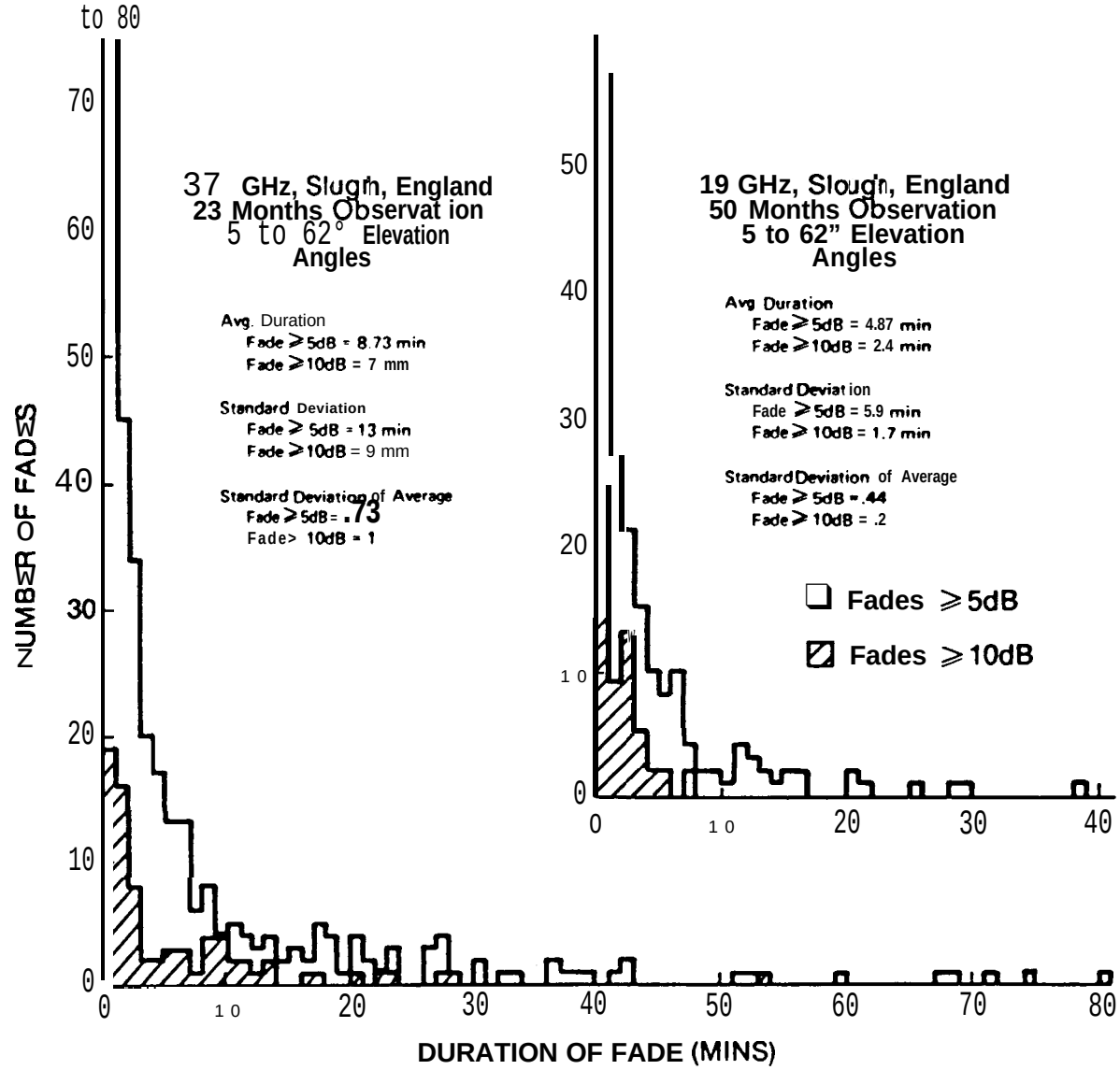

Figure 5.6-2. Histograms of Fades Greater Than 5 and 10 dB at 19 and 37 GHz

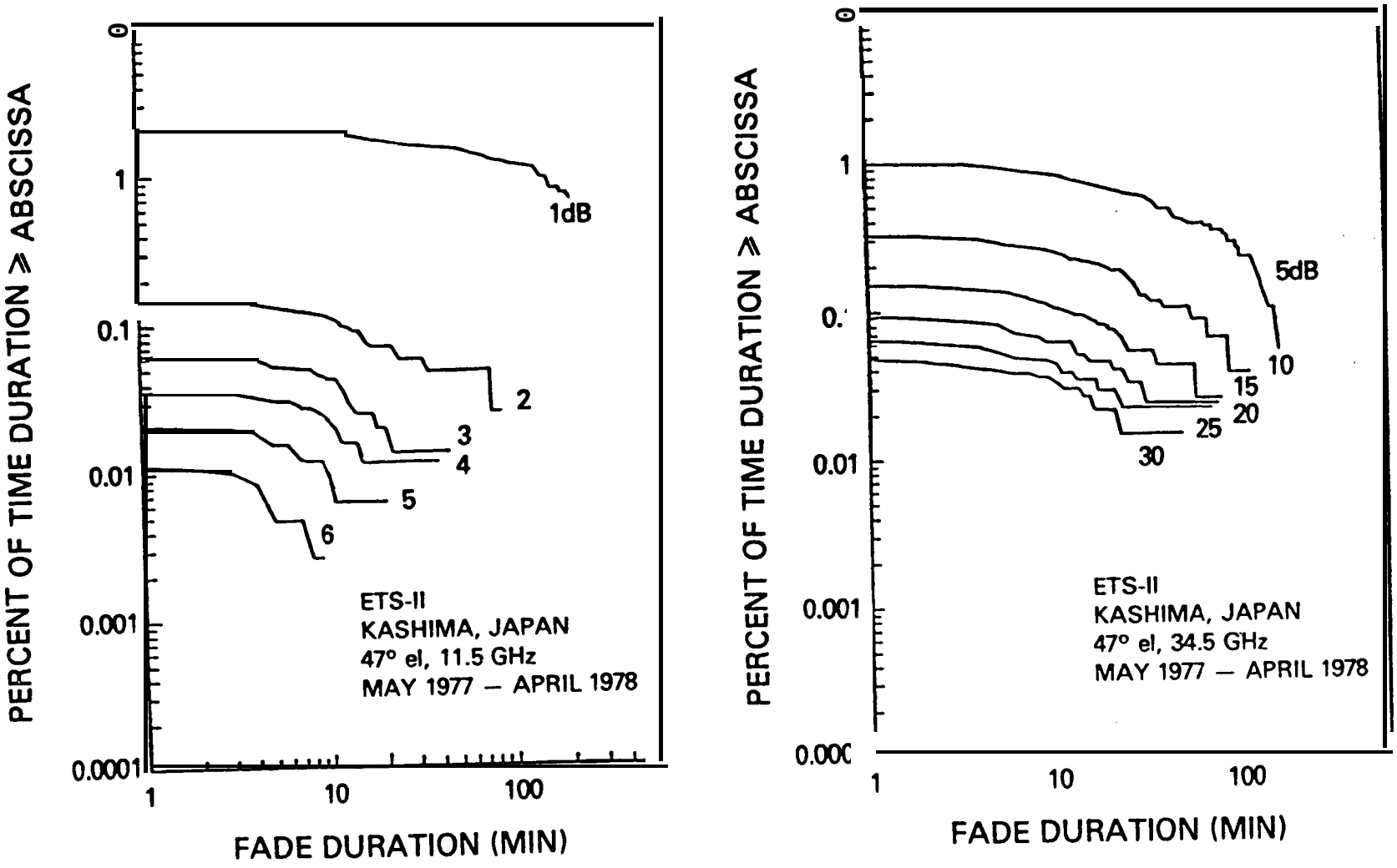

Figure 5.6-3. Fade Duration Statistics for Kashima, Japan, Obtained Using he ETS-II Satellite

5.7.1 19 GHz Data

Figures 5.7-1 and 5.7-2 present the 19 GHz cross-polarization data obtained by the Bell Laboratories experimenters at Crawford Hill, NJ (Arnold, et al - 1979). The near vertical polarization appears to have slightly more cross-polarization discrimination than the horizontal polarization. However, both polarizations show less discrimination than the CCIR estimate. Therefore, in this case, the CCIR approximation appears to be optimistic.

5.7.2 28 GHz Data

The COMSTAR signal at 28 GHz had a fixed polarization, thus allowing measurements at only one orientation with respect to the raindrop anisotropy. The data replotted from Bell measurements (Arnold, et al-1979) is shown in Figure 5.7-3. Again, the CCIR approximation is over-optimistic when compared to the measured data.

5.7.3 Joint Attenuation - Depolarization Data

Systems using orthogonal polarizations for frequency reuse suffer degradation due to crosstalk caused by depolarization in addition to the degradation due to rain attenuation. A full statistical description of the availability of such a system must consider the attenuation and depolarization jointly. Figure 5.7-4 (Arnold, et al - 1979) depicts such joint statistics for attenuation and depolarization on the 28 GHz COMSTAR-Crawford Hill Link. The figure gives the percentage of time that a given attenuation value was exceeded or a given XPD value was not exceeded. Note that the lower bound of all the curves is simply the attenuation exceedance curve, since it corresponds to low values of XPD, which happen a very low percentage of the time. Thus the location of this lower bound is established by attenuation alone. On the other hand, the curves become independent of attenuation for large values of attenuation, since the non-exceedance percentage for XPD far outweighs the exceedance percentage for attenuation.

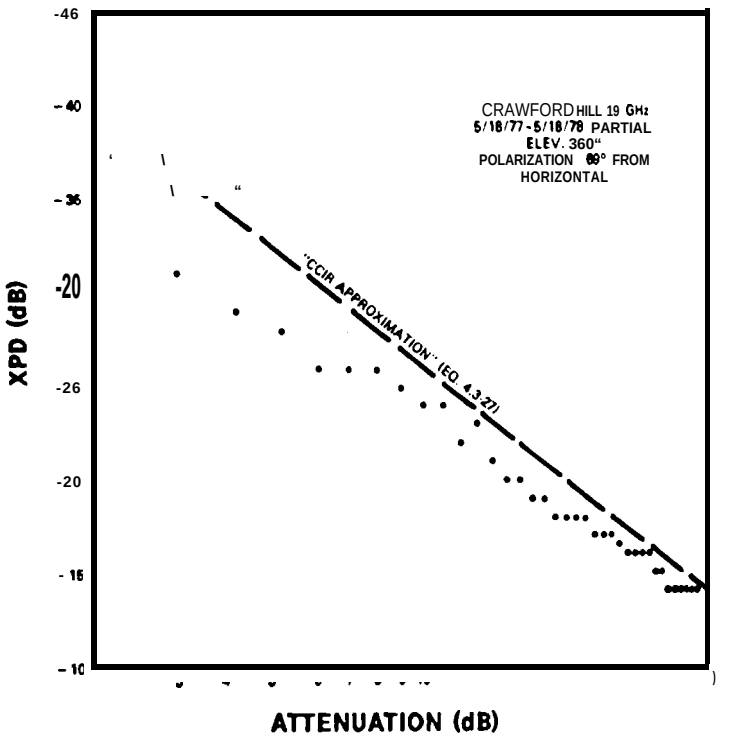

Figure 5.7-1. 19 GHz Cross-Polarization Measurements - Near Vertical Polarization

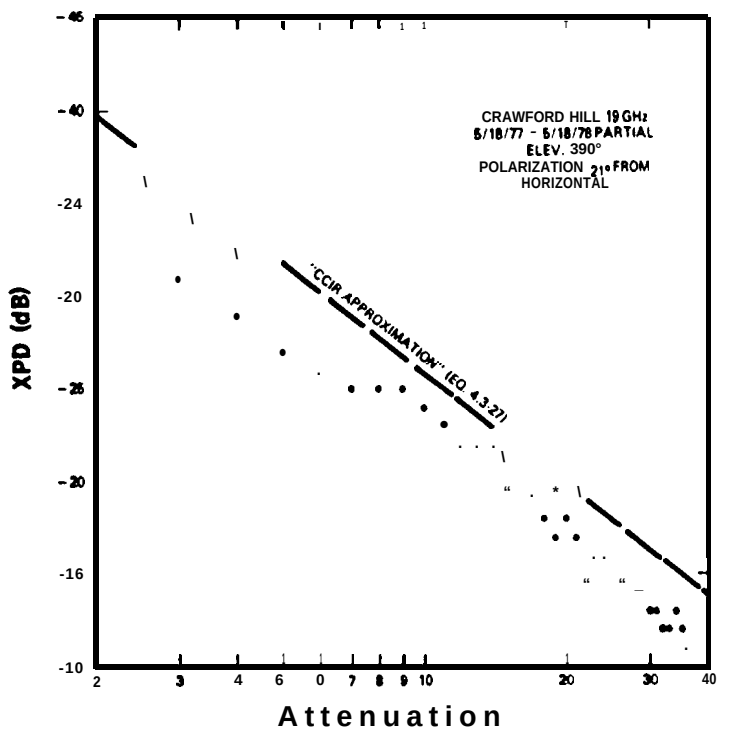

Figure 5.7-2. 19 GHz Cross-Polarization Measurements - Near Horizontal Polarization

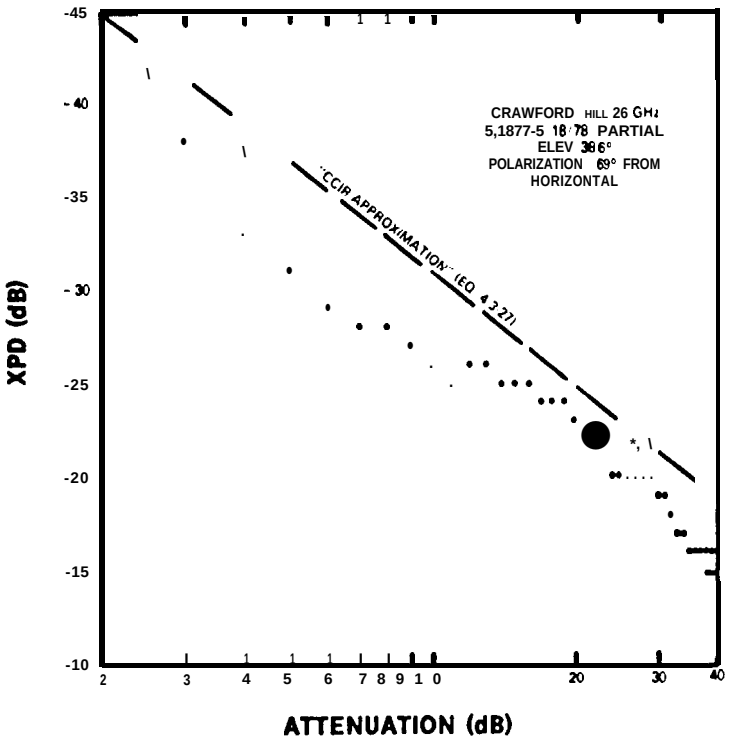

Figure 5.7-3. 28 GHZ Crosspolarization Measurements

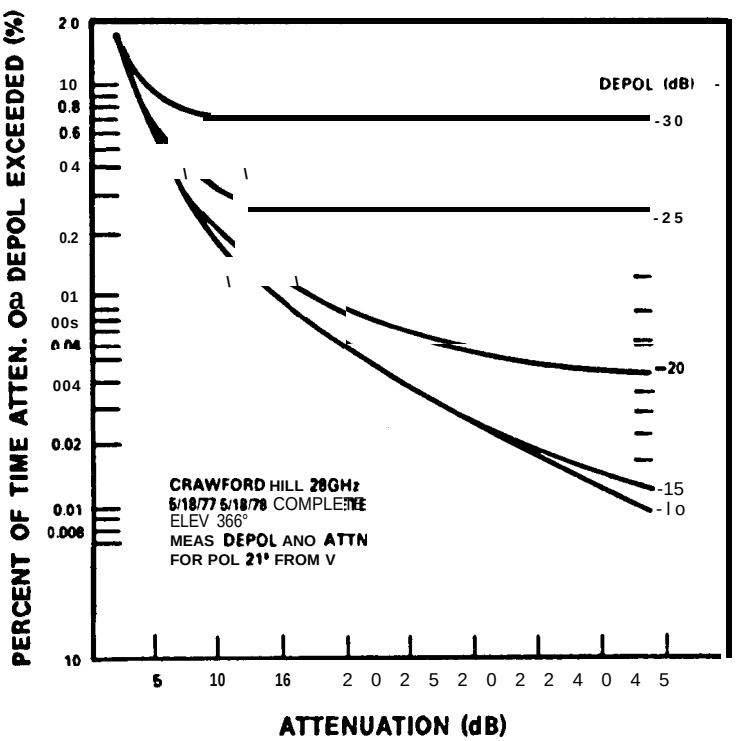

Figure 5.7-4. Joint Attenuation-Depolarization Statistics for 28 GHz Link

A family of curves of the type shown in Figure 5.7-4 gives the outage percentage for a hypothetical system that is unavailable when either an attenuation or an XPD threshold is passed. This is a useful approximation, although most systems allow for some tradeoff between XPD and attenuation. When attenuation is low, for example, greater crosstalk may be tolerable than when attenuation is appreciable.

5.8 PHASE AND AMPLITUDE DISPERSION

Experimental measurements of the phase and amplitude dispersion in the lower troposphere made from the COMSTAR D2 satellite have been made at Crawford Hill, NJ (Cox, et al-1979b). The measurements were made across the 528 MHz coherent sidebands at 28 GHz and between the 19 and 28 GHz carriers which were coherent.

The nine-month Crawford Hill data set has been comprehensively searched for evidence of phase dispersion. For all propagation events, the change in average sideband to carrier phase is less than the measurement uncertainty of about 13° for attenuation up to 45 dB. Phase fluctuations are consistent with signal-to-noise ratios over the 45 dB attenuation range. The change in average 19 to 28 GHz phase is on the order of 60° over a 30 dB attenuation range at 28 GHz. This average phase change appears to be due only to the average dispersive properties of the water in the rain along the path. There is no evidence of multipath type dispersion.

Attenuation in dB at 28 GHz is 2.1 times greater than that at 19 GHz for attenuations up to 29 dB at 19 GHz. The small spread observed in the relationship between 19 and 28 GHz attenuations is consistent with the absence of significant phase dispersion over the 528 MHz bandwidth.

5.9 REFERENCES

Arnold, H.W., D.C. Cox, H.W. Hoffman and R.P. Leek (1979), "Characteristics of Rain and Ice Depolarization for a 19 and 28 GHz Propagation Path from a COMSTAR Satellite," Conference Record, ICC 79, Vol.3,Boston,MA PP 40.5.1-6.

Arnold, H.W., D.C. Cox, and A.J. Rustako, Jr. (1980), "Rain Attenuation at 10-30 GHz Along Earth-Space Paths: Elevation Angle, Frequency, Seasonal and Diurnal Effects, "Conference Record, ICC 80, Seattle, WA, Vol. 3, pp. 40.3.1-7.

Bostian, C.W., et al (1979), "A Depolarization and Attenuation Experiment Using the COMSTAR and CTS Satellites," Virg. Poly. Inst. and State Univ., Annual Report, NASA Cont. NAS5-22577.

Brussaard, G. (1977), "Rain Attenuation on Satellite-Earth Paths at 11.4 and 14 GHz, "URSI Commission F Symposium Proceedings, April 28 - May 6, 1977 La Baule, France.

CCIR (1978) "Rain Attenuation Prediction " Document P/lOS-E, CCIR Study Groups Special Preparatory Meeting (WARC-79), International Telecommunications Union, Geneva.

CCIR (1986a), "Propagation Data and Prediction Methods Required for Space Telecommunications Systems," Report 564-3, in Volume V, Recommendations and Reports of the CCIR - 1986, International Telecommunications Union, Geneva, ISBN No. 92-61-02741-5, NTIS Accession No. PB-87-14116-4.

CCIR (1986b), "Data Banks Used for Testing Prediction Methods in Sections E, F and G of Volume V," Document 5/378 (Rev.1), International Telecommunications Union, Geneva.

Chu, T.S. [1974), "Rain Induced Cross-Polarization at Centimeter and Millimeter Wavelengths," BSTJ, Vol. 53, pp 1557-79.

Cox, D.C., H.W. Arnold and A.J. Rustako, Jr. (1979a), "Attenuation and Depolarization by Rain and Ice Along Inclined Radio Paths Through the Atmosphere at Frequencies Above 10 GHz," Conference Record, EASCON 79, Arlington, VA, Vol. 1, pp 56-61.

Cox, D.C., H.W. Arnold and R.P. Lick (1979b), "Phase and Amplitude Dispersion for Earth-Space Propagation in the 20 to 30 GHz Frequency Range," URSI Program and Abstracts, Spring Meeting, Seattle, Washington, June 18-22, p 253.

Crane, R.K. (1980), "Prediction of Attenuation by Rainr" IEEE Trans. on Comm., Vol. COM-28, No. 9, PPo 1717-1733.

Davies, P.G. (1976), "Diversity Measurements of Attenuation at 37 GHz with Sun-Tracking Radiometers in a 3-site Network," Proc IEEE, Vol. 123, page 765.

Davies, P.G., M.J. Courthold and E.C. MacKenzie (1981), "Measurements of Circularly-Polarized Transmissions from the OTS and SIRIO Satellites in the 11 GHz Band," IEE Conference Publication No. 195, Internat. Conf. Ant. Prop., York, U.K., April 1981.

Fukuchi, H., M. Fujita, K. Nakamura, Y. Furuhama, and Y. Otsu (1981), "Rain Attenuation Characteristics on Quasi-Millimeter Waves Using Japanese Geostationary Satellites CS and BSE," IEEE Conference Publication No. 195, Internat. Conf. Ant. Prop., York, U.K., April 1981.

Goldhirsh, J. (1979), "Cumulative Slant Path Rain Attenuation Statistics Associated with the Comstar Beacon at 28.56 GHz for Wallops Island, VA," IEEE, Trans. Ant. Prop., Vol. Ap 27, No. 6, pp 752-758.

Goldhirsh, J. (1980), "Multiyear Slant-Path Rain Fade Statistics at 28.56 GHz for Wallops Island, VA," IEEE Trans. Ant. Prop., Vol. AP-28, No. 6, pp. 934-941.

Goldhirsh, J. (1982), "Space Diversity Performance Prediction for Earth-Satellite Paths using Radar Modeling Techniques," Radio Science, Vol. 17, No. 6, pp. 1400-1410.

Hayashi, R., Y. Otsu, Y. Furuhama, and N. Fugono (1979), "Propagation Characteristics on Millimeter and Quasi-Millimeter Waves by Using Three Geostationary Satellites of Japan," paper IAF-79-F-281, XXX Congress, International Astronautical Federation, Munich, Germany.

Ippolito, L.J. (1978), "11.7 GHz Attenuation and Rain Rate Measurements With the Communications Technology Satellite (CTS)," NASA Tech. Memo. 80283, Greenbelt, MD.

Kaul, R., D. Rogers and J. Bremer (1977), "A Compendium of Millimeter Wave Propagation Studies Performed by NASA," ORI Tech. Rpt., NASA Contract NAS5-24252.

Kumar, P.N. (1982), "Precipitation Fade Statistics for 19/29 - GHz Comstar Beacon Signals and 12-GHz Radiometric Measurements," COMSAT Technical Review, Vol. 12, No. 1, pp. 1-27.

Lin, S.H., H.J. Bergmann, and M. V. Pursley (1980) "Rain Attenuation on Earth-Satellite Paths - Summary of 10-Year Experiments and Studies," BSTJ, Vol. 59, No. 2, pp. 183-228.

Macchiarella, G. and M. Mauri (1981), "Statistical Results on Centimetric Waves Propagation after Two Years of Activity with the Italian Satellite SIRIO," URSI Commission F Open Symposium, Lenoxville, Canada, May 1980.

Nackoney, O.G. (1979), "CTS 11.7 GHz Propagation Measurements, Third Year's Data and Final Report," GTE Laboratories Report TR-79-471.2, Waltham, MA.

Nowland, W.L., R.L. Olsen and I.P. Shkarofsky, (1977), "Theoretical Relationship Between Rain Depolarization and Attenuation," Electronics Letters, Vol. 13, No. 22, pp 676-7.

Ramat, P. (1980), "Propagation Oblique clans les Bandes de Frequencies des 11 et 14 GHz," URSI Commission F Open Symposium, Lenoxville, Canada, May 1980.

Rice, P.L. and N.R. Holmberg (1973), "Cumulative Time Statistics of Surface Point Rainfall Rates," IEEE Trans. Comm., Vol. COM-21 pp 1131-1136.

Rogers, D. V. (1981), "Diversity- and Single-Site Radiometric Measurements of 12-GHz Rain Attenuation in Different Climates," IEEE Conference Publication No. 195, Internat. Conf. Ant. Prop., York, U.K., April 1981.

Rogers, D. V. and G. Hyde (1979), "Diversity Measurements of 11.6 GHz Rain Attenuation at Etam and Lenox, West Virginia," COMSAT Tech. Rev., Vol. 9, No. 1, pp. 243-254.

Rucker, F. (1980), "simultaneous Propagation Measurements in the 12-GHz Band on the SIRIO and OTS Satellite Links," URSI Commission F Open Symposium, Lenoxville, Canada, May 1980.

Rustako, A.J., Jr. (1979), "Measurement of Rain Attenuation and Depolarization of the CTS Satellite Beacon at Holmdel, New Jersey," 1979 USNC/URSI Meeting, June 18-22, Seattle WA (abstract).

Vogel, W.J. (1979), "CTS Attenuation and Cross Polarization Measurements at 11.7 GHz," Univ. Texas Austin, Final Fpt., NASA Contract NAS5-22576.

Vogel, W.J. (1982), "Measurement of Satellite Beacon Attenuation at 11.7, 1904, and 28.56 GHz and Radiometric Site Diversity at 13.6 GHz," Radio Science, Vol. 17, No. 6, PP. 1511-1520.